1186

9-23-70

SEMI-ANNUAL STATUS REPORT

on

Research Grant NCR 06-002-088

"Electrochemical Studies in Aluminum Chloride Melts"

Grant Period: August 15, 1969 - August 14, 1971

Report Period: February 15, 1970 - August 14, 1970

Principal Investigator

R. A. Osteryoung

Associated Personnel

Dr. Harry Keller

Dr. Larry Boxall (National Research Council of Canada Fellow)

Dr. Janet Osteryoung

Department of Chemistry

COLORADO STATE UNIVERSITY

Fort Collins, Colorado 80521

CONTENTS

Summary

The present study has, thus far, been limited to the equimolar $NaCl-AlCl_3$ system. A relatively simple electrolytic procedure has been developed which appears to give very pure $NaAlCl_4$ melts. Coulometric generation of silver ions has been used to introduce known amounts of silver ion into the melts. By potentiometric measurements, Nernst behavior was shown and a standard potential for the silver-silver ion couple determined. Some preliminary cyclic voltammetry and pulse polarographic measurements were carried out on the Ag-ion/Ag and Pb-ion/Pb electrode systems. The results indicate that the Ag-ion system is a reversible one electron process. Results with Pb-ion are fragmentary, but indicate that Pb(II) has a limited solubility in the melt.

Programs have been developed and debugged which allow pulse polarography with variants and staircase voltammetry with variants to be performed under the control of a Digital Equipment Corporation PDP-8/I computer. Ensemble averaging and digital, least squares smoothing are options within these programs. One program also is capable of automatic peak height and position determination.

An electrochemical circuit has been produced which will operate efficiently under the computerized regimen. It still contains design limitations, and it is reasonable to assume that these can be readily corrected by taking appropriate measures. The limitations involve such things as speed of respond and current output capacity.

A method of driving the two 50-yard coaxial cables connecting the computer and the experiment has been developed and successfully demonstrated. It is anticipated that actual remote experiments will be performed by the end of August, 1970.

Theoretical considerations indicate that the chronocoulometric technique offers advantages over normal potentiostatic methods for the study of electrode kinetics in the fused salt systems.

I. Introduction:

The experimental activity to be carried out under this program has as its goal the study of the electrochemistry of various metal-ion/metal couples in the low melting alkali chloride-aluminum chloride melts.

It is our desire to employ modern electrochemical techniques for the study of electrode reactions at solid electrodes. Techniques such as cyclic voltammetry, pulse polarography and chronocoulometry are to be employed. We seek information on (1) standard potentials of metal-metal ion couples in various aluminum halide-alkali halide mixtures, (2) the chemical species of the solute metal ions in the melt, and (3) kinetic and thermodynamic data for various metal-metal ion couples.

The bulk of this report is divided into two sections. The first deals with experimental work carried out thus far in the fused equimolar $AlCl_3$-NaCl system; the second deals with our efforts to develop a system for the performance of computer controlled electrochemical experiments to be carried out at solid electrodes in the molten salt system in a dry box at a location remote from the computer.

As the bulk of the work requires a well controlled dry-box atmosphere, we have continued our modifications on the Vacuum Atmospheres Dry Box which was obtained just prior to the initiation of the grant period. The nitrogen flowing into the box now is passed through additional water and oxygen removal lines, consisting of a molecular sieve and hot copper, respectively. The box now is sufficiently dry that a broken light bulb operates for at least 6 hours at 110 Volts. Electrical pass-throughs have been installed to permit electrochemical experiments to be carried out in the box. A small furnace, controlled by an externally located temperature controller, is also located in the box. Temperatures to 300°C are possible without excessive heating.

We have found that Fluka (Columbia Organic Chemicals Co., Inc., Columbia, South Carolina - distributor) aluminum chloride appears far more satisfactory than other commercially available material. The "as is" Fluka material was used to prepare a $NaAlCl_4$ melt which is faintly yellow colored and gives electrochemical behavior similar to that reported by Giner and Holleck[1]. Other materials gave much darker melts with various sorts of floating impurities.

II. Theoretical :

Problems inherent in kinetic studies at solid electrodes prompted us to re-evaluate the use of chronocoulometry for the study of electrode kinetics[2]. The results of our considerations indicate that this method is superior to the normal potentiostatic method. By employing charge-time, rather than current-time, studies, measurements at longer times are permitted. Also, a reasonable correction for double layer charging correction can be made. Further, this technique is ideally suited for computer-controlled operation. The results of these considerations were appended to our first Semi-Annual Progress Report, and are in press in Electrochimica Acta[3].

III. Experimental Work in $NaCl-AlCl_3$ Melts:

All of the experimental work was carried out in the nitrogen-filled dry box to protect the melt from moisture and oxygen.

A. Melt Purification.

Previous methods of purification in the literature involved one or a combination of the following steps:

1) preparation of $AlCl_3$ from Al and HCl
2) sublimation of the $AlCl_3$
3) electrolysis using Pt electrodes
4) adding Al or Mg metal
5) filtration

Anders and Plambeck[4] report that after using steps 2 to 5 (cited above), a faint yellow to light brown color remained in the melt.

The fussion of Fluka (A.G., anhydrous, iron free) aluminum chloride and Fulka (A.G.) sodium chloride produced a faintly yellow-colored melt which would slowly turn grey in color on standing for a period of several days. Rather than using a pair of Pt electrodes[5] which produce Cl_2 at the anode during electrolysis, a pair of aluminum electrodes were used. The net result during the electrolysis in the current procedure is either the replacement of impurities in the melt with the aluminum ion or the transfer of Al from one electrode to the other. The simple displacement of the impurities using Al metal failed due to the coating of the metal surface by a film formed by the displaced metal impurities which effectively stopped further replacement. The transfer of Al metal in the electrolysis procedure continually replenishes the Al surface and prevents the passivication of the aluminum. The normal procedure is to electrolyze the melt for ten to twelve hours at a current density of 1.5 ma cm^{-2}.

All the glassware and electrodes were heated to 500°C for several hours and then allowed to cool in the evacuated antechamber of the dry box to prevent any contamination of the melt.

Cyclic voltammetry was used to determine the current-voltage characteristics of the melt before (Figure 1a) and after (Figure 1b)

purification. The final melt was completely colorless and exhibited no irregularities in the current-voltage curves using a tungsten indicator miro electrode. After a week's storage of the melt open to the atmosphere in the dry box, no detectable changes were observed. Hames and Plambeck[4] reported that Pt electrodes are inert in the $NaCl-KCl-AlCl_3$ eutectic. In the $NaAlCl_4$ melt the Pt indicator electrodes were found to be unsatisfactory since polarizations beyond +0.7 volts vs Al(III)/Al produced both anodic and cathodic waves (Figure 1c).

The capacity current, i_c, for the system in the absence of a faradaic reaction is given by:

$$i_c = A C_d v \qquad (I)$$

where A is the indicator electrode area in cm^2, v is the sweep rate in volts per second and C_d is the differential capacity of the double layer in farads per cm^2 at the potential at which i_c is measured. Plots of i, measured at various potentials, versus the sweep rate are shown in Figure 2 and verified the linear relationship as predicted by equation (I) indicating little electroactive impurity. The increase in C_d with a decrease in applied potential (Figure 3) is consistent with the 350 μ F cm^{-2} reported for the aluminum electrode at 0 volts vs Al(III)/Al reference, as deduced from an anodic current step at an Al electrode[6].

The theoretical peak current, i_p, for a reversible system in cyclic voltammetry is given by:

$$i_p = \frac{2n^{3/2}F^{3/2}}{\pi^{1/2}R^{1/2}T^{1/2}} ACD^{1/2}v^{1/2}(0.541) \qquad (II)$$

or

$$i_p = 63.38 \times 10^5 \frac{n^{3/2}ACD^{1/2}}{T^{1/2}} v^{1/2} \qquad (III)$$

at T^oK where

A = area in cm^2

C = concentration in moles cm^{-3}

D = diffusion coefficient

v = sweep rate in volts sec^{-1}

For n = 1, D = 1×10^{-6} cm sec^{-1} and the experimental

conditions in Figure 1b, a millimolal solution of an electroactive solute will produce a theoretical peak current of 1.68 μ A. Cyclic voltammetry is well suited for the detection of the presence of any appreciable amount of reducible impurity in the melt.

B. The Ag(I)/Ag Couple in $NaAlCl_4$ at 200°C.

The Ag(I) was generated coulometrically in a fritted (fine porosity) compartment at a current density of 30 ma cm^{-2}. The overvoltage during the electrolysis never exceeded 200 mv nor did it come close to the point of Cl_2 evolution. The experimental slope of 0.09138 volts from the Nernst plot (Figure 4) is close to the value for the theoretical slope of 0.09388 volts for a one electron change. The standard Ag(I)/Ag potential on the ion fraction scale is 1.262 volts based on a totally ionized melt or 1.233 volts based on a melt in which the ions are Na(I) and $(AlCl_4)^-$.

A typical voltammetric curve from cyclic voltammetry is shown in Figure 5. The expected linear relationship between i and the $(\text{sweep rate})^{\frac{1}{2}}$ and the Ag(I) concentration are shown in Figures 6 and 7, respectively. The extrapolated intercept on the current axis is in rough accord with double layer charging current. The diffusion coefficient for Ag(I) in the melt was estimated, using equation III, to be 0.22×10^{-6} cm sec^{-1}. Melt density was estimated to be 1.70. This value for D is surprisingly small and will be re-investigated. The equation

$$E_p = E^\circ + 1.984 \times 10^{-4} \frac{T}{n} \log [\gamma C] - \frac{7.311 \times 10^{-5} T}{n} \qquad \text{(IV)}$$

which relates the peak potential, E_p, to the standard electrode potential at T°K, was used to calculate a value of 1.068 volts for E°. The discrepancy between the E° calculated from cyclic voltammetry and the E° from the Nernst plot can be attributed to the assumption made in the theoretical derivation of the equations that the activity of the silver metal on the inert indicator electrode is unity at all times. Both the magnitude and the sign of the discrepancy are consistent with the results of Berzins and Delahay[7]. The value of E_p varied

from 0.87 V at v = 0.05 V/sec., to 0.85 V at v = 5 V/sec. and to 0.70 V at 50 V/sec. The shift in E_p indicates that the system is not completely reversible or that the activity of the deposited silver varies materially; however, until the computer is used so that data with a higher degree of reproducibility and precision can be obtained, it is not feasible to pursue the kinetics any further.

A typical integral pulse polarogram and two theoretical curves are given in Figure 8. A maxima which is pronounced in some of the other polarograms produces the difference between the theoretical and experimental curves near the diffusion current plateau. The experimental curve is best approximated by the equation

$$E_i = E_{\frac{1}{2}} + \frac{RT}{nF} \ln(i_d - i) \qquad (V)$$

in which it is assumed that the activity of the silver on the W electrode is unity. The other equation,

$$E_i = E_{\frac{1}{2}} + \frac{RT}{nF} \ln\left(\frac{i_d - i}{i}\right) \qquad (VI)$$

assumes that the silver rapidly forms an alloy with the W and diffuses rapidly into the interior of the W electrode. The expected changes in the diffusion current (Figure 9) and shift in $E_{\frac{1}{2}}$ (Figure 10) with concentration for a one electron change were observed.

The extrapolation of the data for Ag(I)/Ag in the NaCl-KCl-$AlCl_3$ eutectic [4,5] gives an E^o value of 0.810 volts at 200°C. This E^o differs from the E^o in the NaCl-$AlCl_3$ system by 0.452 volts of which only 0.009 volts can be attributed to the change in $AlCl_3$ concentration assuming Nernst ideality. This large shift in potentials can be attributed to the change in the nature of the melt. The chloride activity is drastically altered in the ternary (60 mole % $AlCl_3$) compared to the binary (50 mole % $AlCl_3$) system[8]. The chloride activity is significantly less in the ternary than in the binary system.

Maintaining the 1:1 ratio of the total alkali ion to aluminum ion while changing the total alkali ion content from that of a single ion (e.g., Na, K, Li) to various mixtures would be of interest. It may be possible to correlate shifts in E^o with some parameter such as ion size and to calculate the thermodynamics of the solvent interactions.

The potential of the aluminum electrode as a function of solvent composition can be studied by the use of the cell

$$Al/AlCl_3\text{-}MCl \;//\; AlCl_3\text{-}NCl/Al$$

where M and N represent different alkali metals or mixtures of alkali metals. It has been shown that the liquid junction potential between the two half cells can be estimated using ionic mobilities and that it is usually only a few millivolts[9]. The understanding of the solvent is very advantageous when choosing a solvent for a power system. For example, an increase of about 0.45 volts could be realized in a silver-aluminum cell by merely changing the solvent from the more expensive ternary system to the cheaper binary system. Undoubtedly the kinetics of the various electrode systems will also change with the composition of the solvent.

C. The Pb(II)/Pb Couple in $NaAlCl_4$ at 200°C.

Due to technical difficulties and absence of suitable lead wire electrodes on the commercial market, the lead experimental results are of lower quality and quantity compared to those for silver. The Pb(II) was coulometrically generated in the melt in a similar manner as for silver. The Nernst plot (Figure 11) exhibits a fair proximity of values between the experimental points at low concentrations and the theoretical slope for n = 2. A white crystalline solid formed in the fritted compartment at higher concentrations of Pb(II). The abnormal increase in emf at higher concentrations in the Nernst plot does not indicate that the solid is $PbCl_2$; however, this rapid increase in potential may be a result from a marked increase in the lead activity coefficient.

The cyclic voltammetric curves (Figure 12) exhibited an unusually sharp cathodic peak with an E_p value which varied from 0.64 V at v = 0.5 V/sec., to 0.60 V at v = 5 V/sec to 0.52 V at 50 V/sec. The peak current, i_p, varied linearly with $v^{\frac{1}{2}}$ (Figure 13) and exhibited a sharp break in the linear behavior when plotted against the lead concentration (Figure 14). It is uncertain if

this break occurs at the initial formation of the white solid in the fritted compartment. The behavior is indicative of limited solubility, but is not in agreement with the Pb EMF data. The future use of integral pulse polarography may illuminate the exact meaning of these preliminary results for lead. The E^o for lead, using n = 2 and equation IV, was calculated to be 0.729 volts compared to the 0.903 volts from the Nernst plot (Figure 11). The discrepancy is consistent with that already discussed in the silver results.

IV. System for Computerization of Pulse Polarography for Fused Salts Studies:

A. Purpose:

This portion of the report details the present state of the system being designed to perform computer controlled electrochemistry on fused salts. Results obtained on aqueous chemical solutions are described to indicate the capabilities and limitations of the apparatus presently available. The electronics used, although simple, is discussed since an integral part of the project is the development of remote interfacing between the computer and the experiment. Much of the material contained herein is duplicated in three other documents, "Application of a Computerized Electrochemical System to Pulse Polarography at a Hanging Mercury Drop Electrode", (Appendix I), "Pulse Polarography Program", (Appendix II), and "Staircase Voltammetry Program", (Appendix III). Diagrams in the first of these are referred to in this paper as figures in Appendix I as that paper is considered to be an attachment to this report.

B. Computer Programs:

Each computer program must perform the functions of inputting the experimental parameters, producing the proper waveforms, and taking measurements at the appropriate times. Furthermore, to give maximum utility, the programs should process the data obtained to provide any information of analytical or diagnostic advantage. The first of these functions are fully implemented, but the latter processing function is, as yet, incomplete. Indeed, it is not certain exactly what analytical

and diagnostic measurements are most suitable until the chemical system to be studied is known. A block diagram of the pulse polarography program is given in Figure 2 of Appendix I, as an example of the type of processing that is done in these programs.

Initially the programs must obtain all of the experimental parameters necessary to run the experiment and communicate with the user. This is done in a question-answer mode to make the process easier for the user. Listings of the questions with representative answers are given in Figures 15 and 16. Several of the parameters refer to the voltage waveforms output from the computer. In pulse polarography the waveform is a series of pulses whose width is called the pulse width. They are separated by equal time intervals termed the delay time. Each pulse exceeds in magnitude of that preceding by the step height. The derivative mode pulse polarography waveform is shown in Figure 4 of Appendix I. The output for staircase voltammetry is a staircase shaped pattern. Its parameters are the step height, the step width and the measuring time which must be less or equal to the step width. Figure 17 shows the square wave voltammetry waveform used here. One advantage of the computerized system is the ability to vary the above parameters virtually at will, yet precisely. Custom made instruments frequently fail in this respect.

Although a discussion of what pulse polarography and staircase voltammetry are, and how they are used, might be appropriate at this point, there are sufficient publications on these subjects[10-17].

The experiment may be performed several times, either point repetition as with pulse polarography or repetition of the entire experiment as with staircase voltammetry. The results are then averaged to increase the signal-to-noise ratio. This is known as ensemble averaging or cross-correlation[18,19].

To increase the signal-to-noise ratio still further, digital smoothing of the type recommended by Savitzky and Golay[20] is employed. Peaks are detected and determined by a method similar to that described in their paper.

C. Electrochemical System:

Figure 1 of Appendix I shows a block diagram of the electrochemical system and computer interface. Important features of the system include a voltage divider for the D/A converter output so that the entire 12-bit precision can be utilized, variable capacitance across the Feedback loop of the current follower for optimal stabilization, and a moveable voltage inverter allowing for cathodic or anodic scans. With the exception of these features, the electrochemical instrumentation is of conventional design.

D. Remote Transmission:

Since the computer and drybox are located in distant areas, it is imperative that a means of transmitting information between the two sites be developed. A potentiostat is available beside the drybox and the conversion (A/D and D/A) modules are with the computer so analog transmission was decided upon. The primary problems with this mode are grounding, noise, and signal attenuation. The latter has been handled by two-transistor boosters for matching the line impedance at the driving end (Figure 18). Differential amplifiers at the receiving end boost the signal back to its original level and remove common mode signals. The signal distortion is less than one percent and probably due entirely to the less than perfect common mode rejection of the inexpensive differential amplifiers. The rise time of the five volt square wave test signal after passing through all of the amplifiers is better than 50 microseconds, performance ample for our work.

E. Results:

The kind of results obtainable without the remote feature are shown in Figures 3 and 8 of Appendix I and in Figures 18, 19 and 20. Figure 3 of Appendix I demonstrates the high sensitivity attainable while Figure 8 of Appendix I shows how averaging and smoothing improve the quality of the data. Figure 18 shows how variation of measuring time in integral mode pulse polarography affects the output. Diffusion currents are proportional to the predicted inverse square of the measuring time. Representative staircase and squarewave voltammetry

curves appear in Figures 19 and 20. All four techniques (integral and derivative mode pulse polarography; staircase and squarewave voltammetry) are capable of yielding precise measurements of polarographic half-wave potentials as well as concentrations. Further, parameter variation studies can often provide information on the mechanisms of chemical and electrochemical processes. The fact that staircase and squarewave techniques sweep the voltage in both directions should allow additional information, e.g., on reversibility, to be gathered.

F. Conclusions:

It will be difficult to draw meaningful conclusions about this work until the results of its application to fused salt electrochemistry are known. The computer approach, however, has already shown its promise in the application to pulse polarographic analysis in aqueous media. The output presentation, graphic and especially printed, is more precise than that normally obtainable. Fast sweep experiments have their results plotted on 8½ x 11 paper instead of photographed on Polaroid film. The computer uses simple mathematical algorithms to produce accurate analysis of peaks. It is expected that these features alone will justify the effort expended in developing this computerized electrochemical system.

V. References

1) Giner, Jose and Hollek, G. (Tyco Laboratories, Inc.) "Aluminum Chlorine Battery," Report to NASA, September, 1969, Contract No. NAS-12-688.

2) Christie, J., Lauer, G., and Osteryoung, R.A., J.Electroanal.Chem. 7, 60 (1964).

3) Osteryoung, J.and Osteryoung, R.A., "The Advantages of Charge Methods for the Determination of Kinetic Parameters",Electrochimica Acta - In press, 1970.

4) Hames, D.A., and Plambeck, J.A., Can.J.Chem., 46, 1727 (1968).

5) Anders, U., and Plambeck, J.A., Can.J.Chem., 47, 3055 (1969).

6) DelDuca, B., NASA - TN-D-5503 (Oct. 1969).

7) Berzins, T., and Dalahay, P., J.Am.Chem.Soc. 75, 555 (1953).

8) Tremillon, B., and Letisse,G., J.Electroanal.Chem., 17, 371 (1968).

9) Boxall, L.G., Ph.D. Thesis, Univ. of Sask.,Regina, Canada (1970).

10) Barker, G.C., and Gardner, A.W., A.E.R.E. Harwell, C/R 2297 (1958).

11) Barker, G.C., Faircloth, R.L., and Gardner, A.W., ibid., C/R 1786 (1958).

12) Parry, E.P., and Osteryoung, R.A., Anal. Chem., 36, 1366 (1964).

13) Parry, E.P., and Osteryoung, R.A., ibid., 37, 1634 (1965).

14) Brinkmann, A.A.M., and Los, J.M., J.Electroanal.Chem., 7, 171 (1964).

15) Christie, J.H., and Lingane, P.J., ibid., 10, 176 (1965).

16) Ramaley, L., and Krause, M.S.,Jr., Anal. Chem., 41, 1362 (1969).

17) Barker, G.C., Advances in Polarography, ed. by I.S. Longmuir, Pergamon Press, New York, 1960, p.144.

18) Lee, V.W., Cheatham, T.P., Jr., and Wiesner, J.B., Proc. I.R.E., 38, 1165 (1950).

19) Fisher, D.J., Chem. Instr. 2, 1 (1969).

20) Savitzky, A., and Golay, M.J.E., Anal.Chem., 36, 1627 (1964).

APPENDIX I

Application of a Computerized Electrochemical System to Pulse Polarography at a Hanging Mercury Drop Electrode.

Application of a Computerized Electrochemical System to Pulse Polarography at a Hanging Mercury Drop Electrode.

By H.E. Keller* and R.A. Osteryoung

Department of Chemistry
Colorado State University
Fort Collins, Colorado 80521

*Present address: Department of Chemistry
Northeastern University
Boston, Mass. 02115

BRIEF

Results of applying a computerized pulse polarography system to trace analysis are described. Measurements are made at concentrations as low as 4×10^{-8} M Cd^{++}. The theory required to analyze derivative mode pulse polarography on a hanging drop is developed briefly. Signal averaging and numerical smoothing are used to improve the signal-to-noise ratio.

SUMMARY

Application of computerized pulse polarography on a hanging drop to analysis of extremely dilute solutions is demonstrated. An approximate theory is developed which shows that for reversible systems functionally identical behavior can be expected on the dropping and hanging drop mercury electrodes. A decrease in sensitivity for irreversible reactions would be observed under otherwise identical conditions with the stationary electrode.

Ensemble averaging and digital smoothing are described and their effect on signal-to-noise ratio demonstrated. Variations of pulse height, pulse width and time between pulses are briefly discussed.

Response obtained on 4×10^{-8} M Cd^{++} solution indicates that usable data can be obtained at this level while a precision of 10 percent is indicated on 4×10^{-7} M Cd^{++}.

INTRODUCTION

Derivative mode pulse polarography has been shown to be a very sensitive analytical technique[1,2,3,4]. When performed on a stationary electrode additional advantages may accrue such as increased electrode area[5], increased speed of analysis, and ensemble-averaging[6,7] undisturbed by drop area uncertainty.

Computerization of chemical analysis is becoming very popular today, a fact occasioned by utility and by novelty. In electrochemical analysis, several workers have been engaged in demonstrating the utility of an on-line computer system[6,8,9,10]. By employing a computer to take measurements, control the experiment, and analyze the resulting data, maximum use is made of the advantages of derivative pulse polarography at a stationary electrode. Other capabilities such as convolution of the current response to increase the signal-to-noise ratio and automatic determination of peak positions and heights by a real-time successive approximation technique can be developed readily on a computer system.

In this paper the characteristics of a computerized electrochemical system are described and demonstrated in an application to pulse polarography at a stationary electrode. Some of the advantages of the computer system over conventional systems are developed; some further potential advantages are mentioned.

The realizable sensitivity of the system as an analytical tool seems, at present, to be limited by background. Instrumental artifacts and oxygen appear to be the primary contributors. With the problems, however, measurable response is obtained with 4×10^{-8} M Cd^{++}. Reducing the concentration of supporting electrolyte to below 10^{-3} M is an important factor in this

achievement. This sensitivity compares with stripping analysis where sensitivities as low as 6×10^{-11} M[11] have been reported. More normally values of 10^{-9} M are seen with respect to this technique. It does require that the species determined be concentrated into another phase, a fact which limits its general utility. Potential sweep voltammetry has a reported sensitivity of $\sim 10^{-6}$ M[12] and can be extended by an order of magnitude by analog differentiation[13]. For a discussion of these and other electroanalytical techniques, the reader is referred to reference 14.

EXPERIMENTAL

A PDP-8/I computer (Digital Equipment Corporation) was used for all computing, control, and measurement functions except for the use of a potentiostat and current amplifier, which employed Phibrick-Nexus SP656 and P65AU operational amplifiers. A more complete description of the digital system is given in the next section.

All chemicals were reagent grade and used without further purification. The water was twice-distilled, the first distillation being from alkaline permanganate solution.

A spoutless 100 ml beaker was used as the electrochemical cell. A commercial cover (Beckman Instruments) was adapted to use in this experiment and prepurified nitrogen was always kept flowing over or through the solution. No frits were used in the apparatus.

The indicating electrode was a Brinkmann microburet hanging mercury drop electrode. The capillary was dewetted with dichlorodimethylsilane prior to use and the end broken off. The reference was a Sargent SCE. The auxiliary electrode was a platinum wire separated from the solution by a pin-hole in the end of a piece of glass tubing.

All deaerations were performed for at least 15 minutes. A glass tube with a small hole in the end was used as the nitrogen inlet.

SYSTEM DESCRIPTION

The system, Figure 1, consists of PDP-8/I computer interfaced with a real-time clock, and X-Y plotter, and a potentiostat plus current follower system based on operational amplifiers. All operations are under computer control.

The real time clock can be set under program control to turn on a flag after the passage of from one to 4096 clock pulses or "ticks". This flag is connected to computer skip line so that it may be interrogated by an I/O command. Normally the program uses the skip instruction in a wait loop. The clock can also be read at any time to determine the elapsed time, and it will provide a computer interrupt when the flag is set if the interrupt is enabled. For a more complete description of the clock, see reference 15. Further information on the interface is contained in the article by Lauer and Osteryoung[8].

The plotter is a Hewlett-Packard X-Y plotter with a digital plotting accessory. The two axes are driven by 10-bit D/A converters. Completion of the plotting of a point is signalled to the computer from the plotter.

The electrochemical circuitry is conventional. Input to the potentiostat comes from a variable voltage source and from a 12-bit D/A converter interfaced with the computer. This converter, when properly connected, has a resolution of .5 millivolts for a two volt scan. It is run with a single digital buffer into which information is input from the computer by a jam-transfer method. This method of transfer eliminates the need to clear the buffer before it can receive an input and, therefore, prevents spurious signals during transfer. Switching time of the converter is about 3 μseconds.

The current output from the cell is converted to a voltage through a current follower. The output from this follower is input to a 12-bit A/D converter. This converter has a sample and hold accessory which is activated by program command. The aperture time is 150 nanoseconds while the track time is 12 μseconds. The converter begins conversion on command and gives a conversion complete signal. Conversion time is 35 μseconds. The conversion complete signal may also produce an interrupt if activated.

PROGRAM DESCRIPTION

A block diagram of the program is given in Figure 2. A description of the terms used and certain processes not obvious in the diagram follows.

The experimental parameters are read in a question-answer mode. The clock cycle, voltage division factor, and current measuring resistor values allow time, voltage, and current parameters to be communicated in engineering units rather than in computer internal representation. The voltage division factor is an attenuation between the appropriate D/A converter and the potentiostat. The full 12-bit precision of the D/A converter is only realized if its full scale output of 10 volts can be utilized. Therefore the 10 volt output is divided to result in a control voltage slightly greater than the desired scan range. This division is accomplished by utilizing the fact that the input to the potentiostat is a summing network. Appropriate choice of summing resistor for the D/A input results in the desired scaling.

There are three types of pulse polarography that may be performed. The first, designated N (for normal or integral mode), is produced by maintaining the potential between pulses at a constant value. Each successive pulse is of greater magnitude than the preceding one, and the current response at a fixed time after the application of a pulse is plotted against pulse height. In the D (for derivative) mode, all pulses are of equal height. However, the potential between pulses is stepped to a greater value after each pulse. The current is plotted against the potential prior to application of the pulse. A third mode, Q, has been incorporated to allow the difference between successive pairs of current responses output in the N mode to be plotted. This mode is termed the difference mode. Although the D and Q

modes give functionally identical behavior when used on reversible systems, the fact that the waiting period between pulses is spent at different potenitals can produce marked differences in behavior for systems with complications. An example might be a system exhibiting absroption where desorption would be observed at some potential in the D mode, but since the Q mode would always begin each pluse in the same state it would give no indication of the desorption.

Only in the derivative mode (D), is it necessary to give the value of the pulse height in addition to the other parameters required for all modes.

Delay time is the time between pulses. If a dropping mercury electrode were to be used, the drop would be dislodged at the end of each pulse prior to the dealy time. For plotting, provision is made to input horizontal and vertical tick mark spacings.

During the experiment, the current is measured before and at the end of each pulse voltage which is applied to the electrode. After completion of the requisite number of averaging cycles (pulses) at one potential, the calculated point is plotted and the appropriate digital representation of the potential is incremented.

When the experiment is completed, the stored results may be printed. Also, a digitally smoothed plot may be obtained. If a repeat is desired, it can be made with a change of the plotter vertical amplification factor (a program calculation), the plotter bias (also programmed), and/or the number of averaging cycles simply by answering "Y" (Yes) to the computer's query. For other alterations, the answer must be "N" (No). In the latter case the computer switches are set to indicate the changes desired. The computer will ask for only the parameters selected.

THEORY

Pulse Polarography

An approximate theory of differential pulse polarography is developed here for stationary electrodes. For details, see Appendix II. The results are essentially the same as those derived for derivative pulse polarography at a dropping electrode, and the reader is referred to the original papers for details[16,17,18,19]. The approximate model used here is the application of a potential step from a region of no Faradaic reaction to the potential of interest followed at a time τ by a pulse of height ΔE and duration t. The concentration gradient near the electrode is assumed to be linear when necessary. This assumption should be good for $\tau >> t$.

For "totally reversible" systems, the concentrations of reactant, C_r, and product, C_p, at the electrode surface are determined by the electrode potential, the bulk concentrations, and the diffusion coefficients, D_r and D_p. They are time invariant at any fixed potential. When the Fick's law equations are solved, the concentration gradient prior to pulse application is found to be missing from the expression for Δi.

$$\Delta i = \frac{nFAD_p^{\frac{1}{2}} C_T \gamma^\circ}{\pi^{\frac{1}{2}} t^{\frac{1}{2}}} \qquad \frac{1 - \beta}{(\beta\gamma^\circ + \delta)(\gamma^\circ + \delta)} \qquad (1)$$

See Appendix I for notation. Note that this expression also does not depend on τ and, further, that it is symmetrical about $E_{\frac{1}{2}} + \frac{1}{2}\Delta E$, where $E_{\frac{1}{2}}$ is the polarographic half-wave potential. This is essentially the same expression as those derived previously[16,18]. Derivation of the equivalent equation for a stationary spherical electrode yields the standard spherical correction term for potentiostatic processes[20].

A "totally irreversible" process (see Appendix II) results in an equation containing τ.

$$\Delta i = nFAD_r^{\frac{1}{2}}C_r^{o}(\lambda_o - \lambda)\exp(\lambda_o^2\tau)\mathrm{erfc}(\lambda_o\tau^{\frac{1}{2}})\exp(\lambda^2 t)\mathrm{erfc}(\lambda t^{\frac{1}{2}}) \qquad (2)$$

This equation becomes identical to that given by Barker[15] if ΔE is small and the $\lambda_o^2\tau$ terms are combined with C_r^o. The dependence of τ shows that for long experiments, i.e. the effective value of τ is large, sensitivity to irreversible reactions is decreased. Barker presents the same argument[16]. Note that the concentration gradient again does not appear in the expression. However, higher than first order terms would appear if included in the derivation. Their inclusion would, however, make the mathematics unduly complex.

Therefore, it is important when doing analysis by derivative pulse polarography to try to have the sought after species in a form which displays reasonable electrochemical reversibility at times of the order of the pulse width. A significant corollary to this behavior of irreversible systems is a decrease in the sensitivity to oxygen so that it will cause less interference than in, say, normal (integral mode) pulse polarography.

Signal Averaging.

The theory of cross correlation is well developed[7,21]. Here the cross correlation function is a periodic binary sampling function synchronized with the beginning of each pulse. In effect the result is ensemble averaging. Theory dictates that for random noise, the signal-to-noise ratio will increase as the square root of the number of averaging cycles.

Digital Least Squares Smoothing.

The method of smoothing employed for this paper is that given by Savitsky and Golay[22]. The reader is referred to their paper and references for further details.

RESULTS AND DISCUSSION

Pulse polarograms were run on cadmium nitrate in potassium nitrate supporting electrolyte with the computerized pulse polarography system. The concentrations of cadmium ranged from 4×10^{-5} M to 4×10^{-8} M while the corresponding KNO_3 concentrations were 0.5 M to 0.5 mM. Peak height as a function of concentration is given in Table I. There is an apparent increase of sensitivity at lower concentrations. While the dilutions were made with distilled water thus lowering the ionic strength, resultant double layer effects or migration effects would be expected to be minor. The more likely cause of the loss of linearity is an instrumental one produced by increasing solution and current measuring resistances. With increasing uncompensated resistance, the potentiostat does not control until several milliseconds after the pulse is applied. The peak heights are readily reproducible at all except the lowest concentration where extreme care must be taken to eliminate oxygen. Figure 3 shows the response of the system to the lowest concentration studied, 4×10^{-8} M Cd^{++} in 0.5×10^{-3} M KNO_3. A readily measurable peak is apparent. At higher concentrations a large, well-formed peak is observed. With proper precautions the detection limit for computerized pulse polarography of cadmium should be substantially less than 10^{-8} M. This is better than has been previously reported for pulse polarography.

The reproducibility of the system described in this paper is demonstrated by a series of replicate runs. Data was output on the teletype. The largest value was taken as the peak, while the minimum value preceding the peak was taken as the base line. Four runs at 4×10^{-6} M Cd^{++} had a standard deviation of 1.5% while ten at 4×10^{-7}M Cd^{++} had a standard deviation of 10%.

The drop area was reproducible to only about 1% accounting for most of the error in the first series. Since the background in the second series had a magnitude of roughly one-half of the peak and was not necessarily additive, it is likely that this is the predominant source of error. A longer pulse width than the 20 milliseconds employed plus better electronic circuitry should be sufficient to reduce the error considerably. Better oxygen scrubbing techniques are also indicated.

Effort directed towards optimization of experimental parameters has been reported[4,17]. Because there are new factors present in the hanging drop method and because of the improtance of optimization to achieving maximum sensitivity, certain of these parameters have been investigated here. The parameters associated with the voltage wave form are shown in Figure 4. Calculations were made on the theoretical response for variations of pulse height. There can be no general optimal value since one individual may be concerned with peak separation, while another may desire only a maximum height to half-width ratio. The effect of pulse height on separation has already been discussed elsewhere[4]. The result is that smaller pulse heights provide greater separation at the expense of sensitivity.

Since large pulse height will result in the peak approaching a maximum height while continually broadening and small pulses cause continually diminishing peak height but a constant, minimum peak width, it would seem that some intermediate pulse height should be optimal. An arbitrary measure of the optimal value is the ratio of peak height to the half-peak width. Hand calculations show that this quantity is a maximum when $nF\Delta E/RT = 2.1$ or $\Delta E = 63$ millivolts for a two electron process at 25°C. However, equally significant is the fact that the range of pulse heights allowed if a ten percent variation of the above ratio is permitted is 180/n millivolts to

84/n millivolts at 25°C. It is therefore quite likely that the pulse height for any given experiment will be determined by other factors. This is especially true if two species undergoing reductions requiring different numbers of electrons are being studied simultaneously or if peak separation is a problem.

The actual results of variation of pulse height are shown in Figure 5. The 60 mv curve appears to be the best one. The asymmetry observed at large pulse heights is likely due to insufficient delay times between pulses. At pulse heights of 100 mv and greater, the trailing edge of the peak moves cathodic. However, if there are no nearby interfering ions, then high sensitivity can be achieved by using relatively large pulse heights.

For maximum response the pulse width should be a minimum, although if too short double layer relaxation will make a significant contribution and limit the sensitivity. The effect of pulse widths of 10, 20, and 50 milliseconds is displayed in figure 5. The delay time is ten times the pulse width in each case. The heights obey the $t^{-\frac{1}{2}}$ law predicted by theory to better than five percent. Other experiments show that if the pulse width is greater than .1 seconds, positive deviations are observed. These deviations are readily explained by convection and spherical effects. Much more significant is the effect on the background. The extreme change in the background level observed in Figure 6 is probably due to instrumental limitations. Positive feedback might be capable of reducing this effect thus allowing the instrument to achieve still greater sensitivity.

The delay time between pulses allows for the relaxation of the disturbance. If the delay is too short, then the signal becomes noisy and sensitivity is decreased. Long delays increase measurement time. Therefore the

delay must be a compromise between these effects. For the 50 millivolt pulses used in most of the work a delay of ten times the pulse width was found to be satisfactory. Figure 7 shows the effect of 100 and 200 millisecond delays when the pulse width is 10 milliseconds. A slight sensitivity improvement is observed with the 200 millisecond delay.

One of the primary advantages of a computerized experimental system is the acquisition and storage of data in digital form. This data can then be operated upon during or after the experiment to improve the quality of experimental results. In the present system two means of operating on the data are employed. The data are averaged by taking several measurements at the same potential repetitively, and the data are smoothed by a least squares procedure after the experiment. Both of the operations are optional. The first has the effect of increasing the signal-to-noise ratio as the square root of the number of averaging cycles. There is no distortion created if the delay between pulses is sufficiently long to allow virtually complete relaxation of the disturbance created by the pulses. The second method improves the signal-to-noise ratio as the square root of the number of values over which each point is calculated. Distortion will be introduced if the order of the polynomial used to fit the data is too small to adequately represent the segment of the curve being fit. Test computations indicate that a nine point quartic smooth will introduce no measurable distortion with data points spaced 10 millivolts apart. The two above methods affect the signal-to-noise ratio independently so that the addition of the nine point smoothing algorithm should have the same effect on the signal-to-noise ratio as multiplying the number of averaging cycles by nine. Figure 8 demonstrates the efficacy of

these noise reduction techniques. In Figure 8a a raw curve is shown. Figure 8b shows the effect of averaging over nine cycles while, in Figure 8c, the nine point smoothing routine is used. The two curves show roughly the same reduction in noise. Figure 8d is the result of applying both techniques. The noise is virtually eliminated.

The experimental results indicate that through the use of an on-line computer a significant increase in the sensitivity of pulse polarography can be attained. Particularly important to this increase are the techniques of signal averaging and data smoothing and the ability to vary experimental parameters readily over a wide range.

Legends for figures:

Figure 1: System block diagram

Figure 2: Program block diagram

Figure 3: Derivative pulse polarogram of 4×10^{-8} M Cd^{++}, 5×10^{-4} M KNO_3.
20 cycle average without smoothing. A = .0414 cm^2.
Pulse height = 50 mv. Pulse width = 20 ms. Delay = 200 ms.

Figure 4: Voltage wave form for derivative mode pulse polarography.

Figure 5: Derivative pulse polarograms of 4×10^{-5} M Cd^{++}, .5 M KNO_3.
5 cycle average without smoothing. A = .0414 cm^2.
Pulse height = 20,40,60,80,100,120,140,160 mv.
Pulse width = 20 ms. Delay = 200 ms.

Figure 6: Derivative pulse polarogram of 4×10^{-6} M Cd^{++}, .05 M KNO_3.
5 cycle average without smoothing. A = .0414 cm^2.
Pulse height = 50 mv. Pulse width, delay = 10,100 ms;
20,200 ms; 50,500 ms.

Figure 7: Derivative pulse polarogram of 4×10^{-6} M Cd^{++}, .05 M KNO_3.
5 cycle average without smoothing. A = .0414 cm^2.
Pulse height = 50 mv. Pulse width = 10 ms. Delay = 100,200 ms.

Figure 8: Derivative pulse polarograms of 4×10^{-5} M Cd^{++}, .5 M KNO_3.
Pulse height = 50 mv. Pulse width = 20 ms. Delay = 200 ms.

(a) no smoothing, average x 1 (b) no smoothing, average x 9

(c) 9-pt smooth, average x 1 (d) 9-pt smooth, average x 9

TABLE I

Concentration (M)	Peak height (μa)
4×10^{-5}	57.
4×10^{-6}	7.4
4×10^{-7}	0.92
4×10^{-8}	0.31

ACKNOWLEDGEMENTS

This work was supported, in part, by NASA grant number NGR-06-002-088. Some of the programming ideas are due to George Lauer. The hardware interface was built by P.R. Mohilner and was based on a design for a similar interface by G. Lauer and R.A. Osteryoung. Helpful discussions with J.H. Christie are acknowledged. Contribution number 44-70.

REFERENCES

1. Temmerman, E. and Verbeek, F., J. Electroanal. Chem., 12, 158 (1966)

2. Lagrou, A. and Verbeek, F., ibid., 19, 413 (1968)

3. Parry, E.P. and Osteryoung, R.A., Anal. Chem., 36, 1366 (1964)

4. Peker, C., Herlem, M., and Badoz-Lambling, J., Zeit. fur Anal. Chem., 224, 204 (1967)

5. Christian, G.D., J. Electroanal. Chem., 22, 333 (1969)

6. Perone, S.P., Harrar, J.E.,Stevens, F.B.,and Anderson, R.E., Anal. Chem., 40, 899 (1968)

7. Lee, V.W., Cheatham, T.P. Jr., and Wiesner, J.B., Proc. I.R.E., 38 1165 (1950)

8. Lauer, G. and Osteryoung, R.A., Anal. Chem., 40 (Aug), 30A (1968)

9. Hicks, G.P., Eggert, A.A., and Toren, E.C. Jr., ibid, 42, 729 (1970)

10. Lauer, G., Abel, R., and Anson, F.C., ibid, 39, 765 (1967)

11. Perone,S.P. and Birk, J.R., ibid, 37, 9 (1965)

12. Ross, J.W., DeMars, R.D., and Shain, I, ibid, 28, 1768 (1965)

13. Perone, S.P. and Mueller, T.M., ibid, 37, 2 (1965)

14. Laitinen, H.A., in Trace Characterization, Chemical and Physical, Meinke, W.W. and Scribner, B.F. eds., N.B.S. Monograph 100, U.S. Govt. Printing Office, Washington D.C., 1967.

15. Mohilner, D.M. and Mohilner, P.R., O.N.R. Tech. Report No. 1,Project NR359-493 (July 1969)

16. Barker, G.C. and Gardner, A.W., A.E.R.E. Harwell, C/R 2297 (1958)

17. Barker, G.C., Faircloth, R.L., and Gardner, A.W., A.E.R.E. Harwell. C/R 1786 (1958)

18. Parry, E.P. and Osteryoung, R.A., Anal. Chem., 37, 1634 (1965)

19. Brinkman, A.A.M. and Los, J.M., J. Electroanal. Chem., 7, 171 (1964)

20. Reinmuth, W.H., J. Am. Chem. Soc., 79, 6358 (1957)

21. Fisher, D.J., Chemical Instrumentation, 2, 1 (1969)

22. Savitsky, A. and Golay, M.J.E., Anal. Chem., 36, 1627 (1964)

23. Delahay, P., New Instrumental Methods in Electrochemistry. Interscience, New York, 1954, p. 74.

24. Delahay, P., ibid p. 34

Appendix I: Notation

n = number of electrons transferred per mole of reactant

F = Faraday

A = electrode area

D_r = diffusion coefficient of reactant

D_p = diffusion coefficient of product

C_r & C_p = concentrations

C_r° & C_p° = concentrations at $t = 0$, $x = 0$

$\delta = D_p^{\frac{1}{2}}/D_r^{\frac{1}{2}}$

$C_T = C_r^\circ + \delta C_p^\circ$

$\beta = \exp\ (nF/RT\ \Delta E)$

ΔE = pulse height

$\gamma^\circ = \exp[nF/RT\ (E_i - E^\circ)]$

E_i = potential prior to application of pulse

E° = formal standard potential of electrode reaction

$\lambda_o = k_s D_r^{-\frac{1}{2}} \exp[-\alpha nF/RT\ (E_i - E^\circ)]$

$\lambda = \lambda_o \exp(-\alpha nF/RT\ \Delta E)$

k_s = formal standard heterogeneous rate constant

$\mathrm{erfc}(x) = 1 - \mathrm{erf}(x)$ where $\mathrm{erf}(x) = 2/\pi^{\frac{1}{2}} \int_o^x e^{-t^2} dt$

i = current

i° = current at $t = 0$

$Q = k_s \exp\ [\alpha nF/RT\ (E_i - E^o)]\ \{D_r^{-\frac{1}{2}} + D_p^{-\frac{1}{2}} \exp[nF/RT\ (E_i - E^o)]$

$\mu = \lambda\{1 + \delta^{-1} \exp[nF/RT\ (E - E^o)]\}$

Appendix II

Derivation of Curve Shape for Derivative Mode Pulse Polarography at a Stationary Electrode

From Delahay[23],

$$i = nFAC_r^0 \lambda_0 D_r^{\frac{1}{2}} e^{Q^2\tau} \operatorname{erfc}(Q\tau^{\frac{1}{2}}) \tag{A1}$$

From Fick's diffusion equation, after Laplace transformation and using semi-infinite linear diffusion,

$$\bar{C}_r = C_r^0/s + \bar{a} \exp\left[-x\sqrt{s/D_r}\right] \tag{A2}$$

The new variable, $\bar{a}$, is an undetermined coefficient. Therefore,

$$(\bar{C}_r)_{x=0} = C_r^0 + a \tag{A3}$$

and

$$(\partial \bar{C}_r/\partial x)_{x=0} = -\bar{a}\sqrt{s/D_r} \tag{A4}$$

However, using equation A1,

$$(\partial \bar{C}_r/\partial x)_{x=0} = \frac{\bar{i}}{nFAD_r} = \frac{C_r^0 \lambda_0}{D_r^{\frac{1}{2}}} \frac{1}{s^{\frac{1}{2}}(s^{\frac{1}{2}}+Q)} \tag{A5}$$

Combining equations A4 and A5 yields

$$\bar{a} = -\frac{C_r^0 \lambda_0}{s(s^{\frac{1}{2}}+Q)} \tag{A6}$$

Substituting A6 into A3 and A4 and inverting the transform gives

$$C_r(0,\tau) = C_r^0 - C_r^0\lambda_0 Q^{-1}\left[1 - e^{Q^2\tau}\operatorname{erfc}(Q\tau^{\frac{1}{2}})\right] \tag{A7}$$

and

$$\frac{\partial C_r(0,\tau)}{\partial x} = C_r^0\lambda_0 D_r^{-\frac{1}{2}} e^{Q^2\tau}\operatorname{erfc}(Q\tau^{\frac{1}{2}}) \tag{A8}$$

Similarly,

$$C_p(0,\tau) = C_r^0\lambda_0\delta^{-1}Q^{-1}\left[1 - e^{Q^2\tau}\operatorname{erfc}(Q\tau^{\frac{1}{2}})\right] \tag{A9}$$

and

$$\frac{\partial C_p(0,\tau)}{\partial x} = - C_r^0\lambda_0\delta^{-1} D_p^{-\frac{1}{2}} e^{Q^2\tau}\operatorname{erfc}(Q\tau^{\frac{1}{2}}) \tag{A10}$$

Now, assume that the concentration gradients are linear and can be represented by

$$C_r = c_0 + c_1 x \tag{A11a}$$

and

$$C_p = c_0' + c_1' x \tag{A11b}$$

Once again, solving Fick's equation in Laplace space yields

$$\bar{C}_r = \frac{1}{s}(c_0 + c_1 x) + \bar{b}\exp\left[-x\sqrt{s/D_r}\right] \tag{A12}$$

So that

$$\bar{C}_r(0,s) = c_0/s + \bar{b} \tag{A13}$$

and

$$\frac{\partial \bar{C}_r(0,s)}{\partial x} = c_1/s - \bar{b}\sqrt{s/D_r} \tag{A14}$$

Similarly,

$$\bar{C}_p(0,s) = c_0' + \bar{b}' \tag{A15}$$

and

$$\frac{\partial \bar{C}_p(0,s)}{\partial x} = c_1'/s - \bar{b}'\sqrt{s/D_p} \tag{A16}$$

Substituting into the absolute rate theory expression[24],

$$\bar{i} = nFA\lambda D_r^{\frac{1}{2}}\left\{\bar{C}_r(0,s) - \bar{C}_p(0,s)\exp\left[\frac{nF}{RT}(E - E^0)\right]\right\} \tag{A17}$$

Note that

$$\bar{i} = nFAD_r(\partial C_r/\partial x)_{x=0} \tag{A18}$$

Assume equal and opposite fluxes[23] and use equations A14 and A16 with appropriate manipulation to give

$$\bar{b}' = c_1' D_p^{\frac{1}{2}} s^{-3/2} + c_1 D_r^{\frac{1}{2}} \delta^{-1} s^{-3/2} - \bar{b}\delta^{-1} \tag{A19}$$

Substitute equations A13, A15, and A19 into A17 and A14 into A18; equate currents to get

$$nFA\lambda D^{\frac{1}{2}}\left\{\frac{c_0}{s} + \bar{b} - \left[\frac{c_0'}{s} + \frac{c_1' D_p^{\frac{1}{2}}}{s^{3/2}} + \frac{c_1' D_r^{\frac{1}{2}}}{\delta s^{3/2}} - \frac{\bar{b}}{\delta}\right]\exp\left[\frac{nF}{RT}(E-E^0)\right]\right\}$$

$$= nFAD_r(c_1/s - \bar{b}\sqrt{s/D_r}) \qquad (A20)$$

Solve for $\bar{b}$ using (see Appendix I),

$$\bar{b} = \frac{c_1 D_r^{\frac{1}{2}}}{s(s^{\frac{1}{2}} + \mu)} - \frac{\lambda}{s(s^{\frac{1}{2}} + \mu)}\left\{c_0 - c_0' \exp\left[\frac{nF}{RT}(E-E^0)\right\}\right.$$

$$+ \frac{\lambda}{s^{3/2}(s^{\frac{1}{2}} + \mu)}(c_1' D_p^{\frac{1}{2}} + \frac{c_1 D_r^{\frac{1}{2}}}{\delta})\exp\left[\frac{nF}{RT}(E-E^0)\right] \qquad (A21)$$

Using equations A18, A14, and A21 and inverting the transform

$$i = nFAD_r\left\{c_1 - c_1 e^{\mu^2 t}\operatorname{erfc}(\mu t^{\frac{1}{2}})\right.$$

$$+ \frac{\lambda}{D_r^{\frac{1}{2}}}\left[c_0 - c_0' \exp\left(\frac{nF}{RT}(E-E^0)\right)\right] e^{\mu^2 t}\operatorname{erfc}(\mu t^{\frac{1}{2}})$$

$$\left. - \frac{\lambda}{\mu}(c_1'\delta + \frac{c_1}{\delta})\left[1 - e^{\mu^2 t}\operatorname{erfc}(\mu t^{\frac{1}{2}})\right]\exp\left[\frac{nF}{RT}(E-E^0)\right]\right\} \qquad (A22)$$

Replacing c_0, c_0', c_1, and c_1' with the values given by equations A7, A9, A8, and A10 and subtracting A1 gives

$$\Delta i = nFAD_r^{\frac{1}{2}} C_r^0 \left\{\lambda\left[1 - \frac{\lambda_0}{Q}(1 + \delta^{-1} e^{\frac{nF}{RT}(E-E^0)}) \times \right.\right.$$

$$\left(1 - e^{Q^2\gamma}\operatorname{erfc}(Q\gamma^{\frac{1}{2}})\right) e^{\mu^2 t}\operatorname{erfc}(\mu t^{\frac{1}{2}})\Big]$$

$$\left. - \lambda_0 e^{Q^2\gamma}\operatorname{erfc}(Q\gamma^{\frac{1}{2}}) e^{\mu^2 t}\operatorname{erfc}(\mu t^{\frac{1}{2}})\right\} \qquad (A23)$$

Equation A23 is the general expression for a pulse applied at time τ after a step, using the approximation of linear concentration gradients. The limiting case of a totally irreversible reaction may be obtained from the following limits:

$$Q \longrightarrow \lambda_0, \quad \mu \longrightarrow \lambda, \quad \exp\left[\frac{nF}{RT}(E-E^0)\right] \longrightarrow 0.$$

The result is

$$\Delta i = nFAD_r^{\frac{1}{2}}C_r^0(\lambda - \lambda_0)e^{\lambda_0^2\tau}\operatorname{erfc}(\lambda_0\tau^{\frac{1}{2}})e^{\lambda^2 t}\operatorname{erfc}(\lambda t^{\frac{1}{2}}) \qquad (A24)$$

The limiting case of a totally reversible reaction can be obtained by taking $k_s \longrightarrow \infty$. Then $\mu \longrightarrow \infty$, $\lambda \longrightarrow \infty$ and

$$\lambda e^{\mu^2 t}\operatorname{erfc}(\mu t^{\frac{1}{2}}) \longrightarrow \frac{\lambda}{\pi^{\frac{1}{2}}t^{\frac{1}{2}}\mu}$$

The result is

$$\Delta i = \frac{nFAC_r^0 D_p^{\frac{1}{2}}\gamma^0}{\pi^{\frac{1}{2}}t^{\frac{1}{2}}} \quad \frac{1-\beta}{(\gamma^0+\delta)(\beta\gamma^0+\delta)} \qquad (A25)$$

In the above derivation an electrochemical reduction has been assumed and the initial concentration of the product was zero. In the reversible case the initial concentration of the product may be non-zero and the requirement of linearity of the concentration gradient may be relaxed.

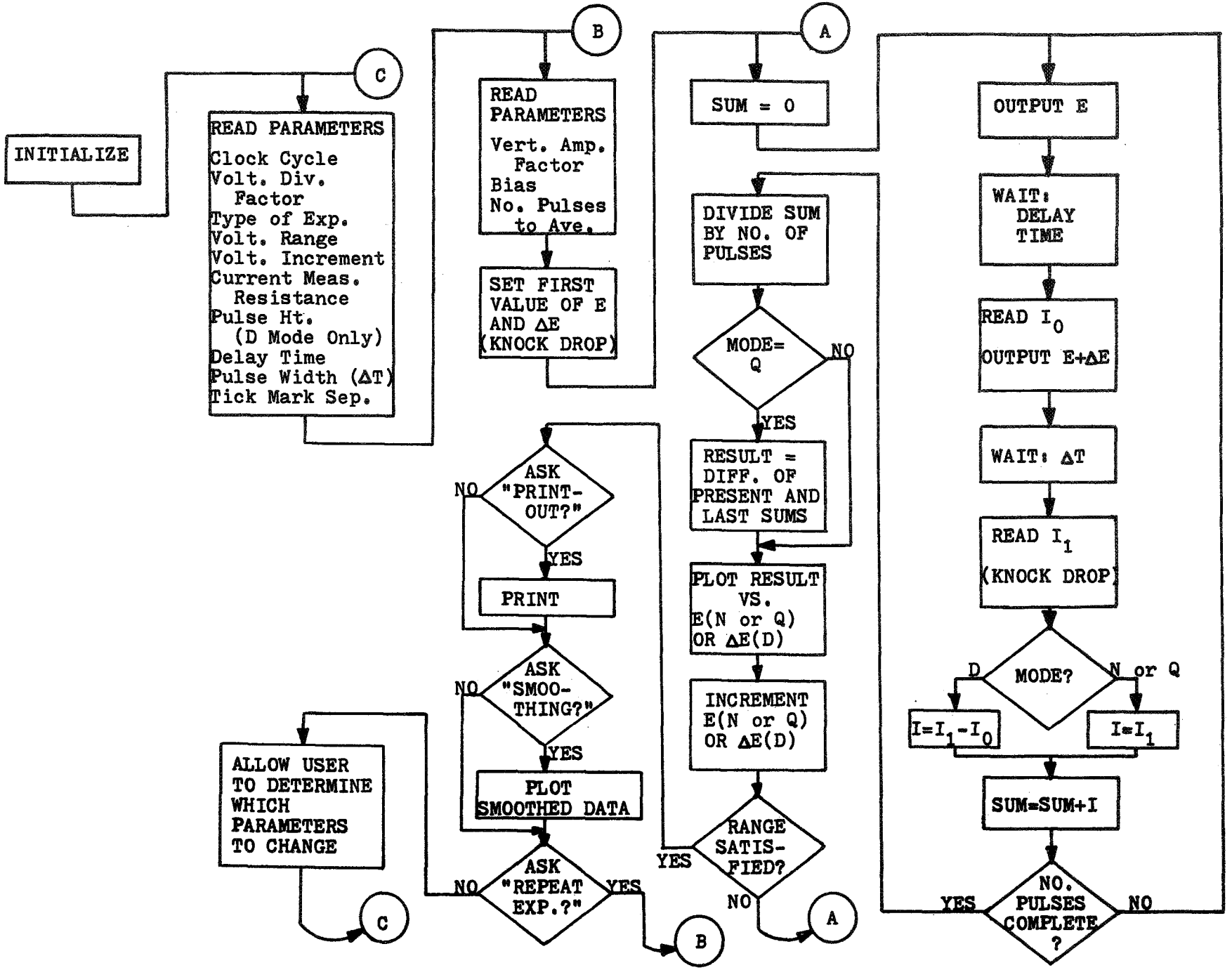
INITIALIZE
C
READ PARAMETERS
Clock Cycle
Volt. Div. Factor
Type of Exp.
Volt. Range
Volt. Increment
Current Meas. Resistance
Pulse Ht. (D Mode Only)
Delay Time
Pulse Width (ΔT)
Tick Mark Sep.
B
READ PARAMETERS
Vert. Amp. Factor
Bias
No. Pulses to Ave.
SET FIRST VALUE OF E AND ΔE (KNOCK DROP)
A
SUM = 0
DIVIDE SUM BY NO. OF PULSES
MODE= Q
NO
YES
RESULT = DIFF. OF PRESENT AND LAST SUMS
PLOT RESULT VS. E(N or Q) OR ΔE(D)
INCREMENT E(N or Q) OR ΔE(D)
RANGE SATIS-FIED?
YES
NO
A
OUTPUT E
WAIT: DELAY TIME
READ I_0
OUTPUT E+ΔE
WAIT: ΔT
READ I_1 (KNOCK DROP)
MODE?
D
N or Q
$I=I_1-I_0$
$I=I_1$
SUM=SUM+I
NO. PULSES COMPLETE ?
YES
NO
ASK "PRINT-OUT?"
NO
YES
PRINT
ASK "SMOO-THING?"
NO
YES
PLOT SMOOTHED DATA
ASK "REPEAT EXP.?"
NO
YES
B
ALLOW USER TO DETERMINE WHICH PARAMETERS TO CHANGE
C

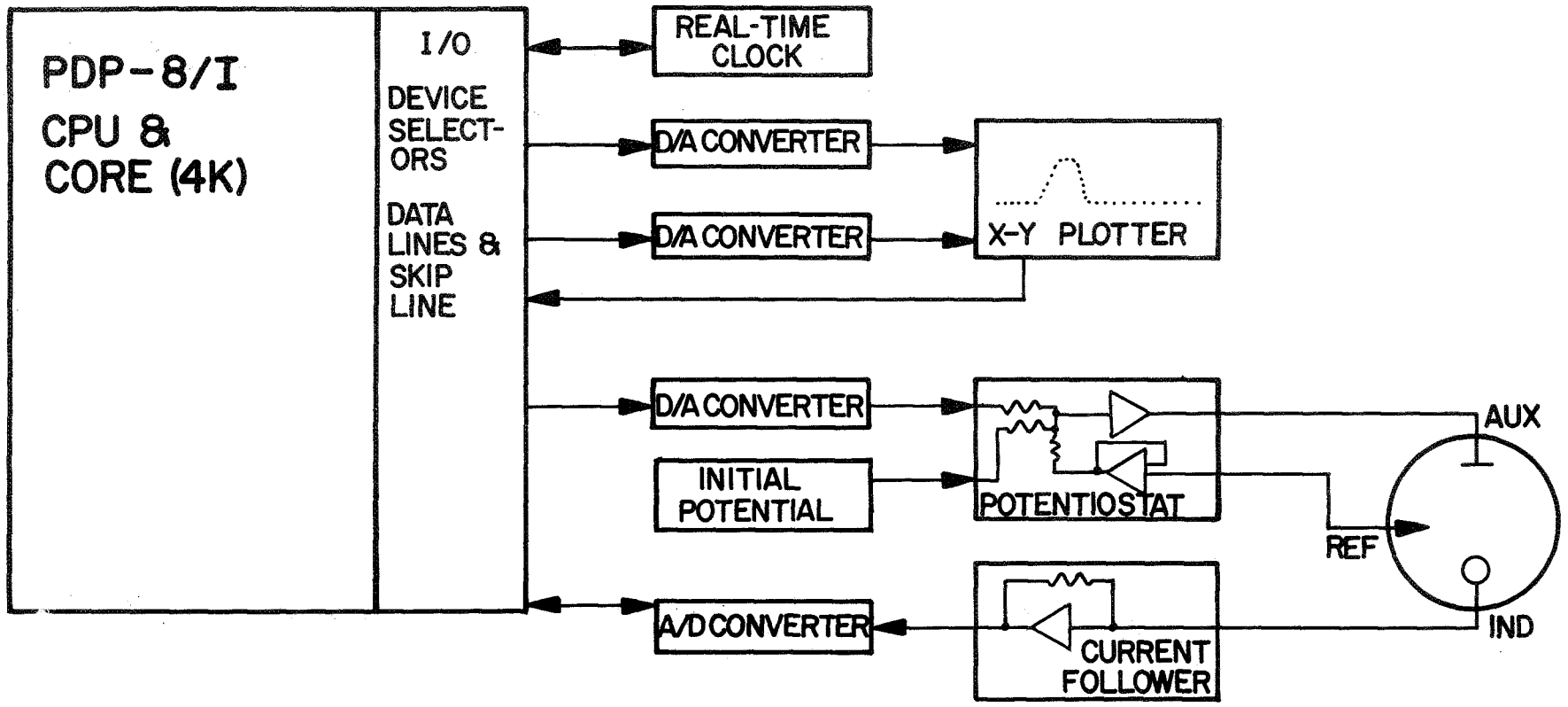
PDP-8/I
CPU &
CORE (4K)
I/O
DEVICE
SELECT-
ORS
DATA
LINES &
SKIP
LINE
REAL-TIME
CLOCK
D/A CONVERTER
D/A CONVERTER
X-Y PLOTTER
D/A CONVERTER
INITIAL
POTENTIAL
POTENTIOSTAT
AUX
REF
IND
A/D CONVERTER
CURRENT
FOLLOWER

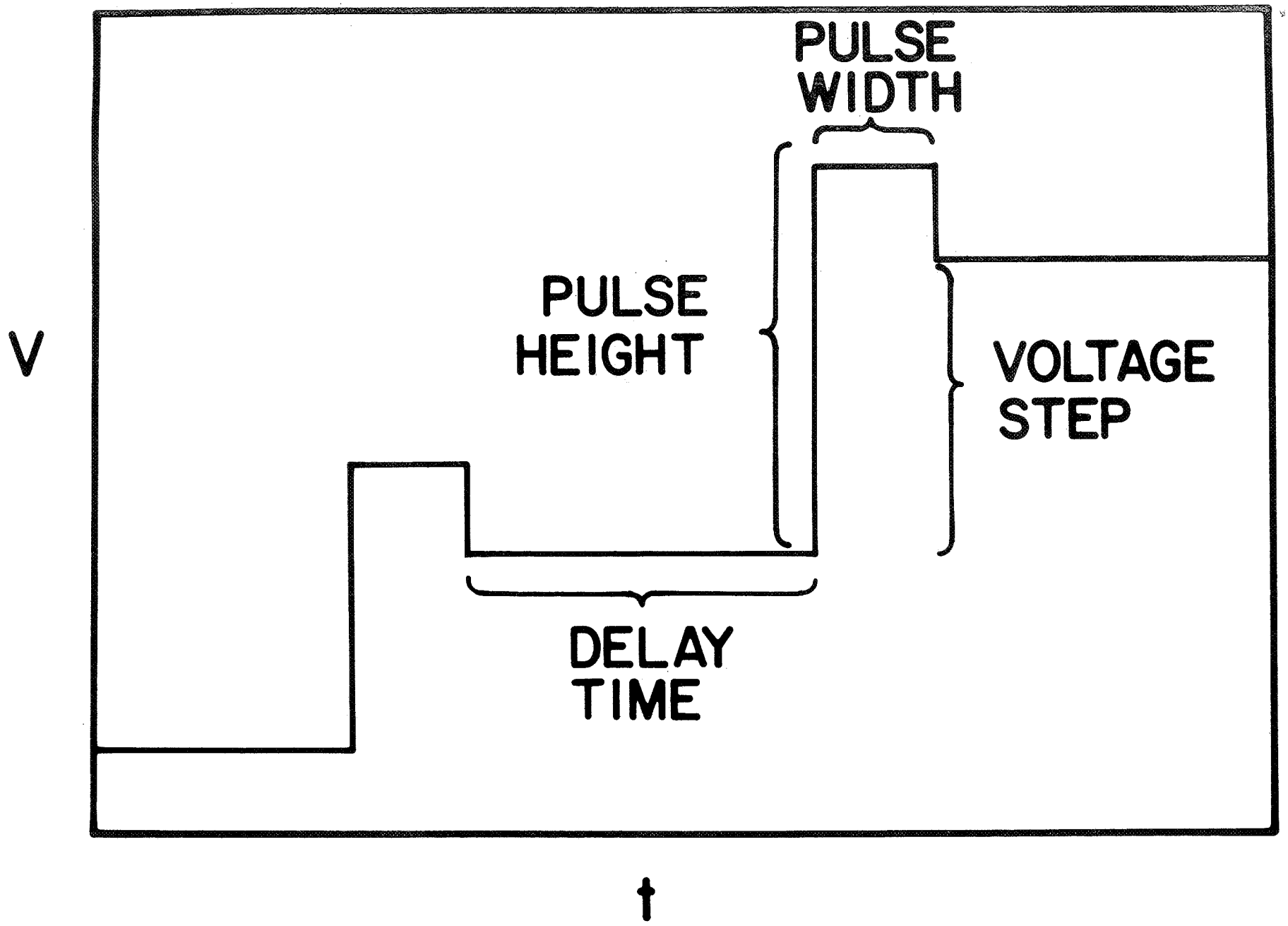
PULSE
WIDTH
PULSE
HEIGHT
VOLTAGE
STEP
DELAY
TIME
V
t

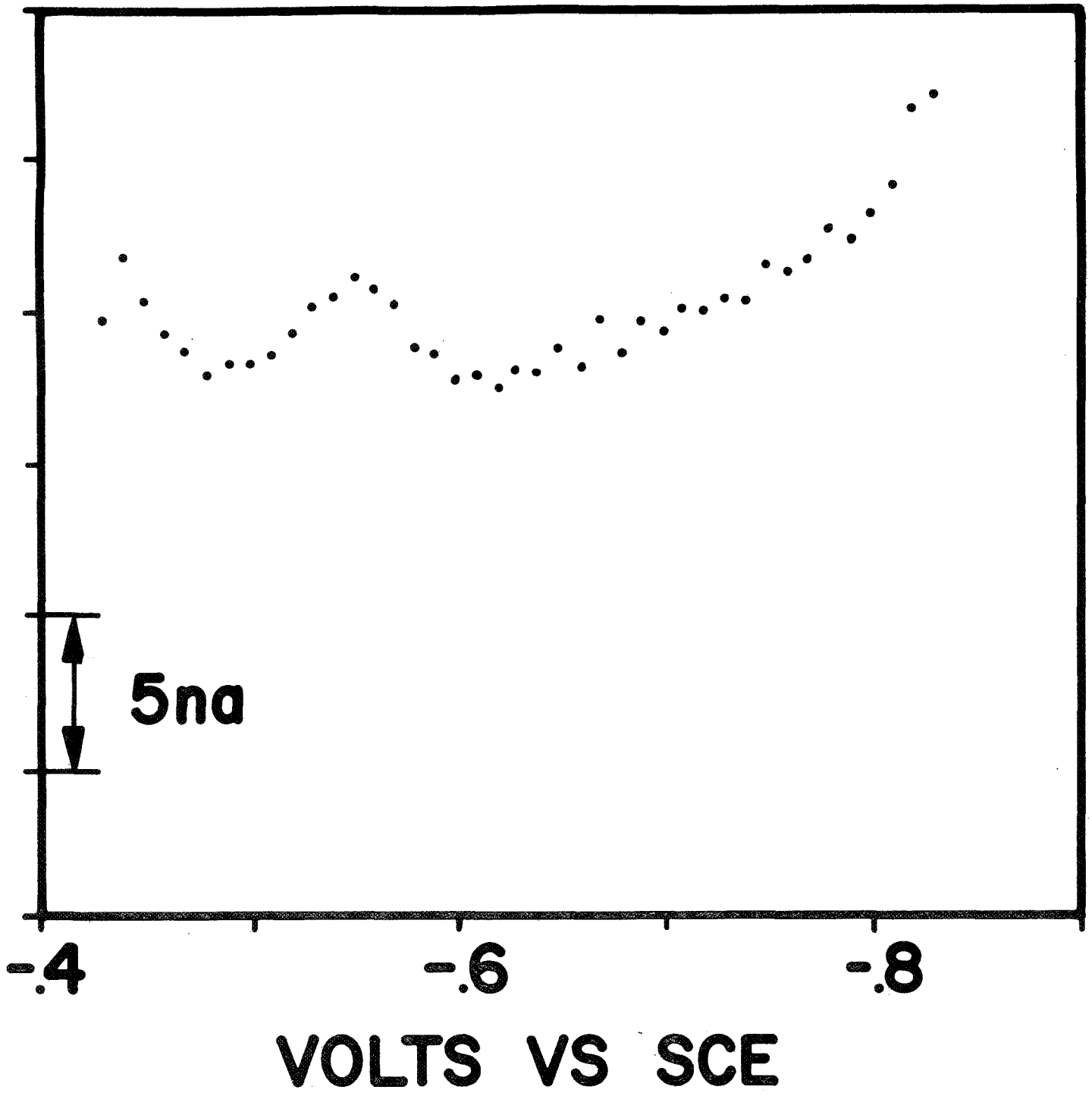
5na
-.4
-.6
-.8
VOLTS VS SCE

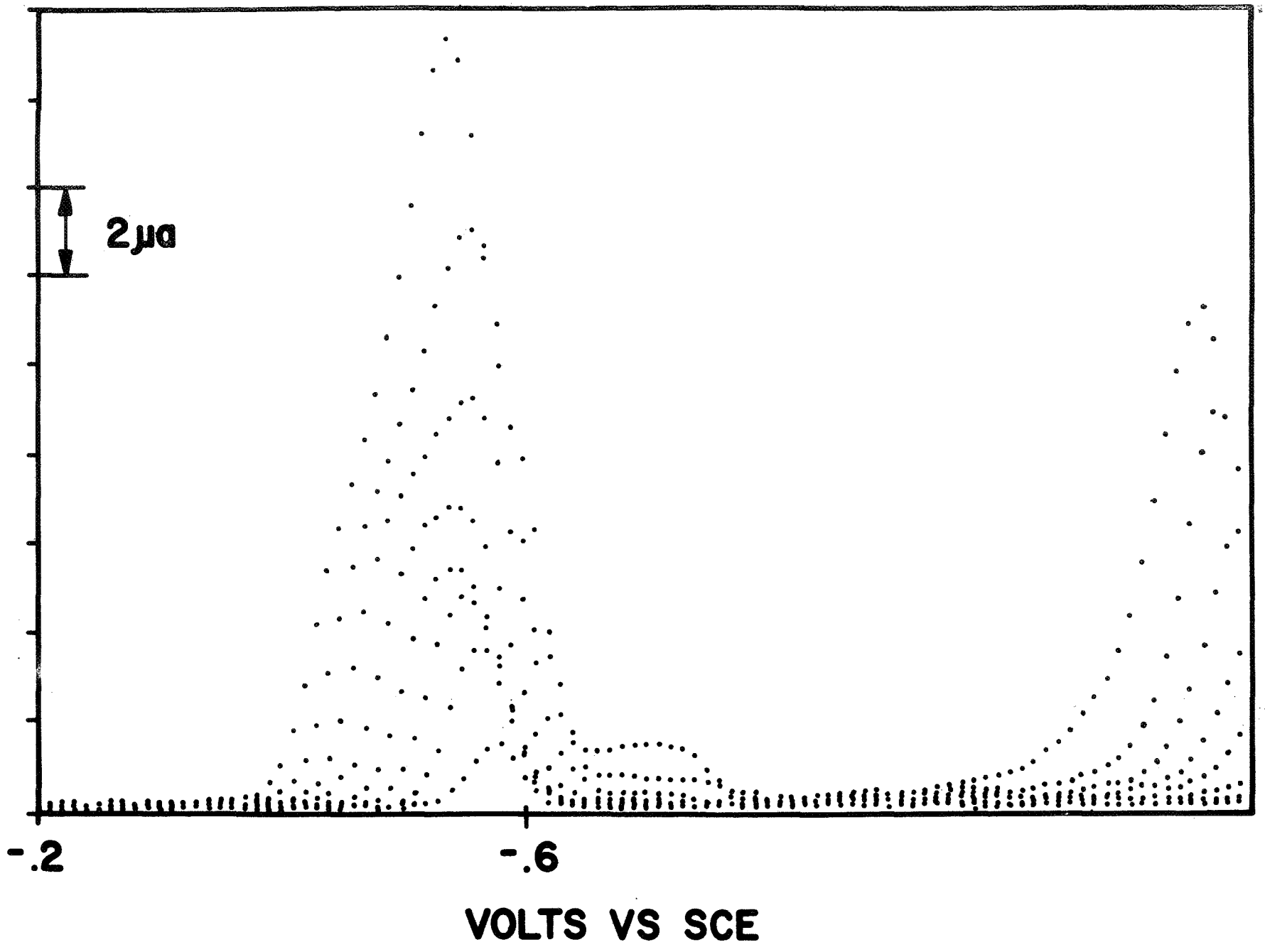
2 μa
-.2
-.6
VOLTS VS SCE

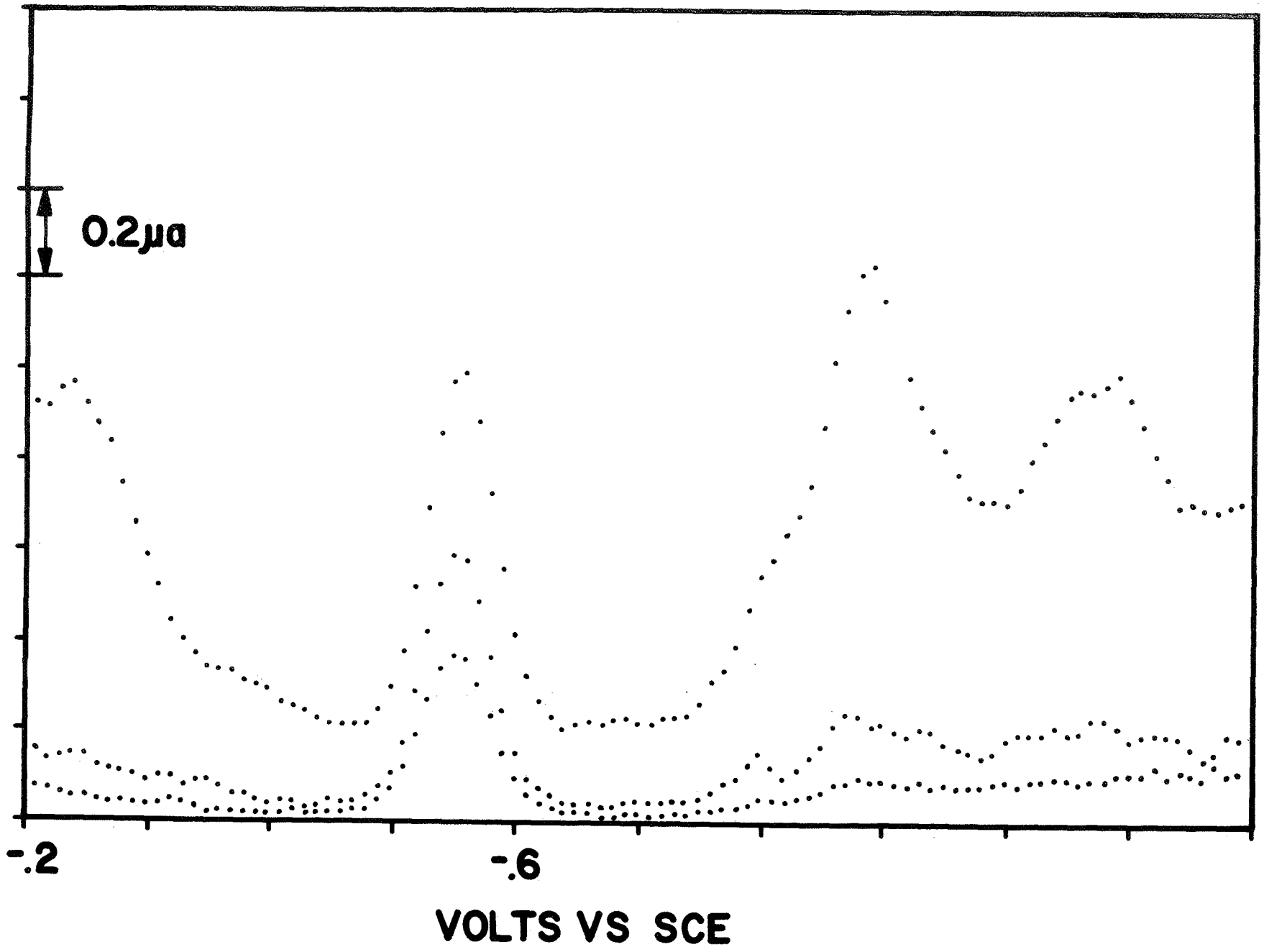
0.2μa
-.2
-.6
VOLTS VS SCE

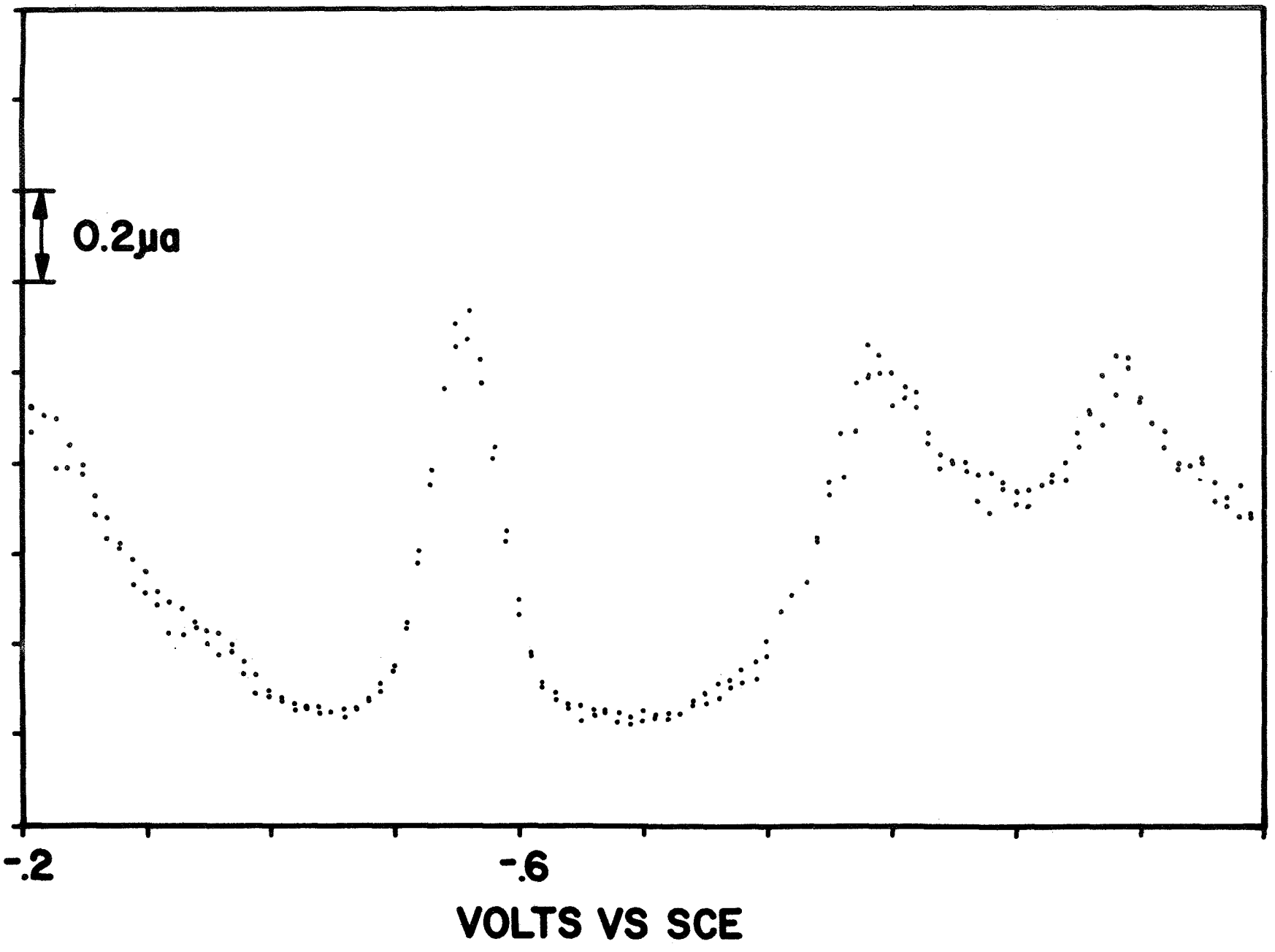
0.2μa
-.2
-.6
VOLTS VS SCE

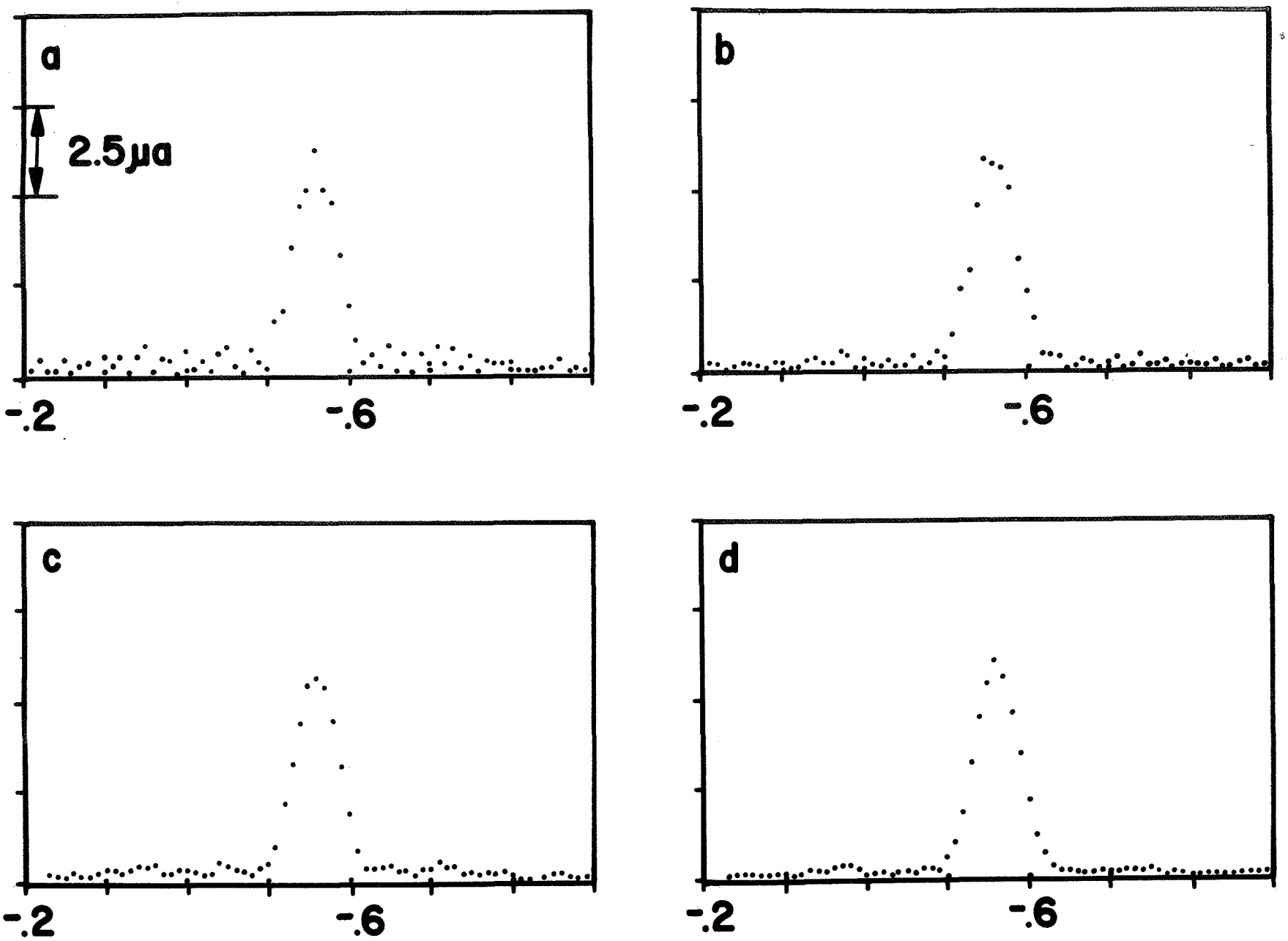
a
2.5μa
-.2
-.6
b
-.2
-.6
c
-.2
-.6
d
-.2
-.6
VOLTS VS SCE

APPENDIX II

Pulse Polarography Program

PULSE POLAROGRAPHY PROGRAM

By H. E. Keller

July 24, 1970

I. Purpose

The pulse polarography program is designed to produce the voltage waveforms required, collect appropriate data, and analyze the data collected. There are a large number of parameters and options in the program. This report explains their use.

II. Waveforms and Hardware

Two output waveforms are available in the present program. One is for operating in the normal or integral mode. The other is used in derivative mode pulse polarography. The first waveform consists of a sequence of pulses from a zero base line. A pulse of a given height is repeated if averaging of more than one value is desired. The average number is input on the teletype when requested. After the requisite number of duplicate pulses have been output, the magnitude of the pulse height is increased by a parameter called increment (step height). This sequence continues until the pulse height reaches the value of the range. The experiment is then complete. The width of the pulses is input as the pulse width, while the time from the end of one pulse to the beginning of the next is the delay time.

Note that current measurements are made prior to and at the end of each pulse and that after the latter current measurement the drop knocker, if connected, is activated.

In the derivative mode the pulses are of constant height, the pulse height, and appear on a staircase base line. The height of each step in the base line is the step height. All other parameters retain their same meaning. The experiment is complete when the base line magnitude is equal to the range.

The hardware required to operate the pulse polarography program consists of a normal potentiostat-current measuring system with a few minor modifications. The potentiostat input resistor from the D/A converter should be variable to divide down the D/A output voltage. If the voltage follower input resistor is 10K, then a 50K D/A resistor will result in dividing the 10 volt range of the D/A converter to a 2 volt potentiostat range, an output voltage division factor of 5.

One further change is necessary. The D/A on our PDP-8/I outputs from 0 to -10 volts. This output must be inverted for anodic scans. In addition, the program is designed to accept positive-going current signals. Therefore, if a current follower is used, the output must be inverted when using cathodic scans.

III. Loading the Program

The program can be loaded either from the disk or from tape. In either event, the floating point package must also be loaded. This package is usually on the disk, but may also be obtained on paper tape. The preferred method of loading is use of the disk loader which requires use of the disk monitor system.

To obtain the disk monitor, load 7600 in the switch registers, press "stop," press "load add,", press"start." A period will appear on the teletype. Type LOAD followed by a carriage return. The computer will print IN-. If the program is on the disk (named PP4) type S:FFP2,S:PP4 followed by a carriage return. FFP2 is the present name of the floating point package, but it may change in the near future. If you wish to load the program from tape, type S:FFP2,R:. The tape should be mounted in the high speed reader. It will be read twice. Next the computer will type one asterisk on each of two lines signifying the legitimacy of the input files and then type OPT-. Type 2 indicating a two-pass load is desired. The computer will type ST=; you type 200 followed by a carriage return. Now an up arrow will appear. Respond to each up arrow (there will be

six) by typing control P. Pause after the tape is read (if you are using tape input) to reload the tape. The program will start automatically.

IV. Parameters and Options

Once the program is started, either by loading or through transfer to location 200, it will make a series of inquiries to determine the experimental parameters that the user wants for the next experiment. Most of the parameters correspond to switches on the switch register so that later changes can be made selectively. All times are in milliseconds, all potentials in volts, and all currents in microamps. All numerical entries are made in standard floating format.

The first parameter requested is the clock cycle or period. Its exact value can be determined through a clock calibration program available separately. There is no corresponding register switch.

Next, the output voltage division factor is asked for. This parameter is described in section II and sets the maximum voltage range available. This parameter corresponds to switch 0.

The computer then asks for the experiment type. The letter N indicates normal, D is for derivative (see section II), while O stands for difference mode. In this last mode, a normal (N) experiment is run, but differences between successive data points are output instead of the data points themselves. Use switch 1 for this parameter.

Switch 2 corresponds to the three parameters in the next question, the current measuring resistor (R_M), the voltage scan range, and the voltage increment. The first of these is the ratio of the voltage output to the A/D converter and the current through the cell. The other two are explained in Section II. The value of the current measuring resistor is used to compute the full scale current on the

plotter (full scale is -10 volts out of the Y axis D/A converter).

If in the D mode, the next query (switch 3) is to determine the pulse height described in Section II. Next the delay time and pulse width (switch 4) are input.

For the purpose of setting up the plotter the pen is next moved to the upper right and lower left corners. The zero adjust is used first (upper right), then the variable gain (vernier) is adjusted. Switch 5 controls this operation. Switch 6 provides the tick marks. The tick mark spacing is requested.

The D/A is now set to zero volts and periodic pulses of interval equal to the delay time are provided to the drop knocker. Thus the initial potential may be set and proper operation of the drop knocker ascertained. These operations are indicated with switch 7.

The final values input are controlled by no switch and so must be input for every experiment. These are the plotter vertical scale factor, the plotter vertical bias, and the average number. The first of these is simply an internal digital multiplier while the second is an internal digital additive term. They allow the plotted curve to be expanded and moved up or down to increase sensitivity and suppress the base lines. These parameters are also significant to the peak determination routine.

The average number is the number of times pulses are repeated for the potential plotted. The responses are summed and divided by the average number.

After the run is complete, the program asks if a printout (in micro-amps) of the curve is desired. If answered yes, the computer prints the curve one current value to a line. Should the user wish to discontinue printing, he need only set switch 11. Next, the program asks if the user wants the output smoothed (using a nine point quartic least squares fit). Should the reply be affirmative, a new

piece of paper is assumed to be in the plotter so that new axes are drawn. Each point is then printed and plotted beginning with the fifth point. If switch 11 is set, printing is suppressed. Now the user is asked whether he wishes a peak determination scan to be made. In this, the program rejects any peak less than one-fifth of the plotter scale as plotted. Therefore it considers the bias and scale factor in this rejection feature although they do not appear in the printed value for peak height (in micro-amps). The peak position is displayed in volts assuming the initial potential to be zero.

The experiment and data evaluation now complete, the next question is whether to repeat. If the response is yes, then only the scale factor, bias, and average number may be changed. If the reply is no, then the switches may be set to indicate additional changes to be made.

V. Experiment Setup

No particular potentiostat system will be assumed here. It is necessary to be able to pre-bias the cell control voltage, to divide the D/A output before it reaches the cell, and to provide a voltage in the range -5 to +5 volts proportional to the current.

The potentiostat is connected to the cell, the D/A (6054) connected through an appropriate dividing system to the E-control input of the potentiostat, and the I-cell output of the potentiostat joined to the A/D converter input. The clock must be in the "op" position and the plotter connected properly.

If the drop knocker is to be used, the clock pulse output should be jumpered to the solenoid control connector. The drop knocker is attached to "solenoid out."

VI. The Program

In order to read out and understand the program, a few facts are required. First, the instruction mnemonics have been somewhat

expanded. This expansion takes two forms, I/O instructions and non-I/O. The mnemmonics for the added I/O instructions are given in the following table:

Mnemonic	Octal	Meaning
ZCLKR	6701	Direct clear holding register.
SETCLK	6702	Strobe AC into holding register
RDCLK	6704	Read (logical or) holding register into A.C.
ZCTR	6504	Clear clock counter.
CLKSTR	6712	Start clock.
CLKSTP	6714	Stop clock.
SKCLK	6311	Skip on clock flag.
CCLKF	6312	Clear clock flag.
ADSF	6531	Skip on A/D flag.
ADCV	6532	Sample, hold, and begin A/D convert.
ADBR	6534	Read A/D register into AC and clear flag.
DA1	6501	Strobe AC to D/A #1.
DA2	6502	Strobe AC to D/A #2
DA3	6503	Strobe AC to D/A #3.
ENSOL	6772	Enable solenoid (drop knocker)
DISOL	6774	Disable solenoid.

The remaining (non-I/O) mnemonics were instituted to make the program shorter, easier to read, and easier to translate to another machine. They are described in the following table:

Mnemonic	Equivalent	Octal	Comments
CALL	JMS I	4400	Used to call a subroutine.
RET	JMP I	5400	Used to return from a subroutine.
FENTER	JMS I 7	4407	Enter floating point package.
FEXT	-----	0000	Leave floating point mode.
PUTF	DCA 45	3045	Used before FLOAT command.
GETF	TAD 45	1045	Used after FIX command.

Additional floating point package interpreter mnemonics are

described in other documentation. The features of the PALD assembler used here are completely discribed in the PALD assembler manual.

The program is organized so that the control of parameter input and the actual running of the experiment are done by the main program. There are subroutines for message writing, timing, plotting, and various computational and post-execution operations. These subprograms are mnemonically named, and should not require a detailed explanation of their operation.

APPENDIX III

Staircase Voltammetry Program

STAIRCASE VOLTAMMETRY PROGRAM

By H. E. Keller

Introduction:

This program is intended to generate a staircase-type voltage waveform for application to an electrochemical cell through appropriate potentiostatic circuitry. It will measure the response of the chemical system at a fixed time during each step. The results of the experiment are plotted and, optionally, printed as current versus applied voltage. An option is available to allow square wave voltammetry[1] to be performed. The results of one complete voltage cycle are output.

---

[1] L. Ramaley and M. S. Krause, Jr., Anal. Chem., 41, 1362 (1969).

Auxiliary Equipment:

The auxiliary equipment required consists of a potentiostat with variable control potential attenuation and a current-to-voltage transducer (current follower). Input voltage (control voltage) will always be between 0 and -10 volts, and scans will begin in the negative direction. Therefore, provisions for inverting and biasing this voltage are essential if maximum versatility is to be obtained. The output from the current follower must be in the range -5 to +5 volts in order to eliminate clipping.

Operation:

After loading and starting the program, a dialogue between user and computer ensues. This dialogue consists of questions posed to the user and his responses. Most of the questions are numbered to correspond to the PBP- /I console switches. After completion of an experiment, the computer provides the query "Do you wish to repeat exp?" If the answer is "Y" (yes), the experiment is immediately repeated. Should the user reply "N" (no), the computer then directs the user to "set switches for

changes in setup" and "press key." The user then sets the console switches corresponding to the changes he desires to make. Only those statements selected in this manner will be typed out by the computer. After the switches are set, any operational key pressed on the teletype will direct the computer to inquire for responses corresponding to the selected switches. A sample teletype conversation is included. Most of the questions and responses are self-explanatory. The following notes describe terms which may be uncertain.

Output voltage division factor: This is the control potential attenuation of the potentiostat.

RM: The measuring resistor of the current follower.

Full scale current is...: The computer provides this information so that the plot may be calibrated. Notice that the scale factor will affect the vertical plot scale.

Type of exp.: N= staircase voltammetry, S= square wave voltammetry.

Range: The span of voltage to the cell (after attenuation).

Step HT: Size of voltage steps.

Pulse HT: Used only in mode S, size of pulse added to step during first half of step.

Meas time: Time after beginning of step when current measurement is made. Must be step width in mode N, one-half step width in mode S.

Set X & Y full scale: Adjust plotter pen to upper right corner using zero control.

Set X & Y to zero: Adjust plotter pen to lower left corner using gain controls.

SC MKS: Scale marks. Ticks will be placed at desired intervals.

Current scale factor: Multiply current by this number before plotting.

I bias: Normally zero is at the bottom of the plotter. This variable provides the capability of moving the zero up (or down) by the amount given.

Several error messages are provided. If any value typed in is illegally zero, the computer will type "try again." Other messages signal excessive

range, illegal experiment type, and measuring time too large. While the experiment is running, some messages may also be emitted. If any teletype key is depressed (and the teletype is on), the experiment will be stopped and the message "interrupted" typed. If the experiment is being run too rapidly for the A/D converter, the message "too fast" is typed. Should either of these two cases arise or if the experiment is completed normally, "Do you wish to repeat exp?" is typed.

The voltage and current values at each point will be printed if switch 11 is not set before the completion of the experiment. As soon as it is set, printing will cease. Switch 10 will cause punching of those numbers on the high speed punch.

If an input to the A/D converter is out of range, no point will be plotted. Similarly, if a point would be plotted below the bottom of the paper, it is suppressed. No attempt is made to distinguish between the forward and reverse scans on the plotter.

Description of the Program:

After all of the necessary parameters are read in, converted to usable values, and, in some cases put into fixed form, the interrupt is turned on and the experiment begun. Just prior to beginning the experiment, a number of initializations are performed. Location 11 (an auto-index register) is set to the address of the beginning of storage minus one. This register will contain the last location into which a (raw) current has been stored. Location 12 is similarly initialized and holds the address of the last current plotted. Hence, the content of location 11 is referred to as the store pointer, while 12 is the plot pointer. All device flags (including teleprinter) are cleared. The timing sequence pointer ("JMP I TMAD"in location "TMJMP") is initialized. Various variables are set to their beginning values.

At this point the clock must be set. If more than 4095 ticks are required for the first time interval, it is set to zero, giving the maximum of 4096 ticks before a clock pulse occurs. The clock counter is

zeroed, automatically setting the clock flag which is then cleared. The appropriate value is placed in the D/A3 (control potential) register, interrupt turned on, and the clock started. At this point the machine goes into a wait loop testing whether a point is to be plotted. The test is made by comparing the store and plot pointers. If the former is greater than the latter, then a point may be plotted and the plot routine is entered.

When the first time interval is ended, an interrupt occurs and the clock flag is set. The interrupt causes a transfer to the interrupt handler via location 1. The return address is saved in location 0. The interrupt handler saves the AC and link. This saving is done here to save space in the handler. It would be efficient to save the AC and link only if necessary. A skip chain is performed to determine the nature of the interrupt with the clock receiving highest priority.

If the interrupt is from the teletype keyboard, the experiment is interrupted and the program recycled. A message is printed.

If any interrupt other than clock, A/D, or keyboard occurs, all flags that could have caused it are reset and the experiment continues.

If the interrupt was caused by the A/D converter, then the number is fetched and stored in the next location indicated by the incremented store pointer if it is to be stored. Otherwise (mode 5) it is held in a temporary location. A flag is set to -1 (ADFL) and the restore sequence performed. This sequence restores the machine to its state prior to the interrupt jump.

If the interrupt is a clock interrupt, a check is made to see if the entire time interval is over. This may require many interrupts as the clock can only count to 4096. If the interval is not complete, appropriate action is taken and the restore sequence entered. If the time interval is completed, the timing sequence pointer is incremented and a jump made through it. Separate actions take place

depending on where the machine is in the timing sequence. At the end of the first time interval (TMSA*4096+TMSB) a check is made to see if ADFL = -1 (initialized to -1 before experiment is begun). If it is not, the experiment is running faster than the A/D converter. An error message is issued and the program recycled. A flag (AFLAG) is set to 0 for the first interrupt (to -1 for the third timing interval). Next, the A/D conversion is started and the clock set to the next interval (PWIDA*4096+PWIDB). The restore sequence is entered.

At the end of the second timing interval (possibly identical with the first), a determination is made of the mode. If the mode is N, then this is the last interval. Otherwise a new voltage is output through D/A3, the clock set to the measuring interval and the restore sequence entered. The third interval is handled in the same way as the first except that AFLAG is set to -1. This flag determins the action of the A/D interrupt routine in mode S.

At the interrupt from the last timing interval, the timing sequence pointer is reset, and a test is made for the end of the sweep. If the test fails then the D/A holding registers are incremented, a new voltage is output through D/A3, a new clock setting is made, and the restore sequence is entered. If the end of the first sweep is detected appropriate actions are taken to reverse the sweep and the test for the end of sweep. If the reverse sweep is complete, the registers determining sweep direction are restored and the clock stopped. In either event, the restore sequence is entered.

When the plot routine determines that all of the points have been plotted, the print routine is entered. At this point smoothing and peak determination options (to be implimented) are made available. The program is then recycled.

Note that much information regarding the operation of this program is contained in the pulse polarography program write-up and has not been duplicated here.

Addendum:

The program has been modified to do signal averaging. Several entire experiments are run and the results averaged. The number of runs is called the average number. If the average number is greater than one, a wait time is requested. This is the time between runs in milliseconds. The maximum time is roughly 16,000,000 times the clock period.

FIGURES

Figure 1: Cyclic Voltammetry in the $NaAlCl_4$ melt at 200°C
Sweep rate = 0.5 volts/sec.

1a: Before purification
W indicator electrode

1b: After purification
W indicator electrode

1c: After purification
Pt indicator electrode

Figure 2: Cathodic current vs. sweep rate
System = $NaAlCl_4$
Temperature = 200°C
Area of W indicator electrode = 0.817 mm^2
A - measured at 0.4 volts vs. Al(III)/Al
B - measured at 1.0 volts vs. Al(III)/Al

Figure 3: Differential capacity using a W electrode in $NaAlCl_4$ vs. Applied Potential
Temperature = 200°C

Figure 4: Nernst Plot at 200°C for the cell:

$Al/NaAlCl_4//Ag(I)$ in $NaAlCl_4/Ag$

The concentration scale is based on a totally ionized melt (cation fraction)
Least squares slope = 0.09138 volts
Nernst slope (n=1) = 0.09388 volts
E^o_x = 1.2618 volts
Based on the melt composition $Na^+ (AlCl_4)^-$ (mole fraction scale)
E^o_N = 1.2330 volts

Figure 5: Cyclic voltammetric curve of Ag(I) in $Na(AlCl_4)$ at 200°C.
W indicator electrode
Sweep rate = 0.5 volts/sec.
Mole fraction Ag(I) = 1.44×10^{-2}

Figure 6: Cathodic peak current vs. $(\text{sweep rate})^{\frac{1}{2}}$
Mole fraction Ag(I) in $Na(AlCl_4)$ = 2.224×10^{-2}
W indicator electrode area = 0.817 mm^2
Temperature = 200°C

Figure 7: Cathodic peak current vs. Ag(I) Concentration
Sweep rate = 10 volts/sec.
W indicator electrode area = 0.817 mm^2
Temperature = 200°C

Figure 8: Integral pulse polarogram of Ag(I) in $Na(AlCl_4)$ at 200°C
Mole fraction of Ag(I) = 1.222×10^{-3}
W indicator electrode area = 0.817 mm^2
Melab Pulse Polarograph
Delay time = 1.5 sec.
Step height = 5.33 mv
Average x1
Pulse width = 100 ms
Measure time = 66 ms

A - experimental curve
B - $E = k_1 + \frac{RT}{F} \ln (i_d - i)$

C - $E = k_2 + \frac{RT}{F} \ln \frac{(id - i)}{i}$

D - pure solvent

Figure 9: Diffusion current vs Ag(I) concentration
Temperature = 200°C
W indicator electrode area = 0.817 mm^2

Figure 10: Variation of $E_{\frac{1}{2}}$ with Ag(I) concentration
Temperature = 200°C
W indicator electrode area = 0.817 mm^2
Nernst slope (n=1) = 0.09388 volts
Least squares slope = 0.08778 (n=1.07)

Figure 11: Nernst plot at 200°C for the cell
$Al/NaAlCl_4$ // Pb(II) in $NaAlCl_4/Pb$
The concentration scale is based on a totally ionized melt (cation fraction)
Using Nernst slope as drawn (n=2)
E^o_x = 0.9028 volts
Based on the melt composition $Na^+(AlCl_4)^-$, (mole fraction scale), and Nernst slope (n=2)
E^o_N = 0.8740 volts

Figure 12: Cyclic voltammetric curve of Pb(II) in $Na(AlCl_4)$ at 200°C
Sweep rate = 1 volt/sec
W indicator electrode area = 0.817 mm^2
Mole fraction Pb(II) = 3.104×10^{-3}

Figure 13: Cathodic peak current vs. $(\text{sweep rate})^{\frac{1}{2}}$
Mole fraction Pb(II) in $Na(AlCl_4)$ = 9.336×10^{-3}
W indicator electrode area = 0.817 mm^2
Temperature = 200°C

Figure 14: Cathodic peak current vs. Pb(II) concentration
Sweep rate = 10 volts/sec.
W indicator electrode area = 0.817 mm^2
Temperature = 200°C

Figure 15: Questions and answers for Pulse Polarography

Figure 16: Questions and answers for Staircase Voltammetry

Figure 17: Squarewave Voltammetry Waveform

Figure 18: Line Driver Circuit Diagram

Figure 19: Integral mode pulse polarography
0.18mm Cd(II) Delay Time = 500 ms
0.20mm Pb(II) Step height = 10 mv
0.5M KNO_3 Average x5

Figure 20: Staircase Voltammetry
0.18mM Cd(II) Step width = 25 ms
0.20mM Pb(II) Measure time = 25 ms
0.5M KNO_3 Step height = 10 mv
Average x5

Figure 21: Square wave voltammetry
0.18mM Cd(II) Step width = 50 ms
0.20mM Pb(II) Measure time = 25 ms
0.5M KNO_3 Step height = 10 mv
Pulse height = 50 mv
Average x5

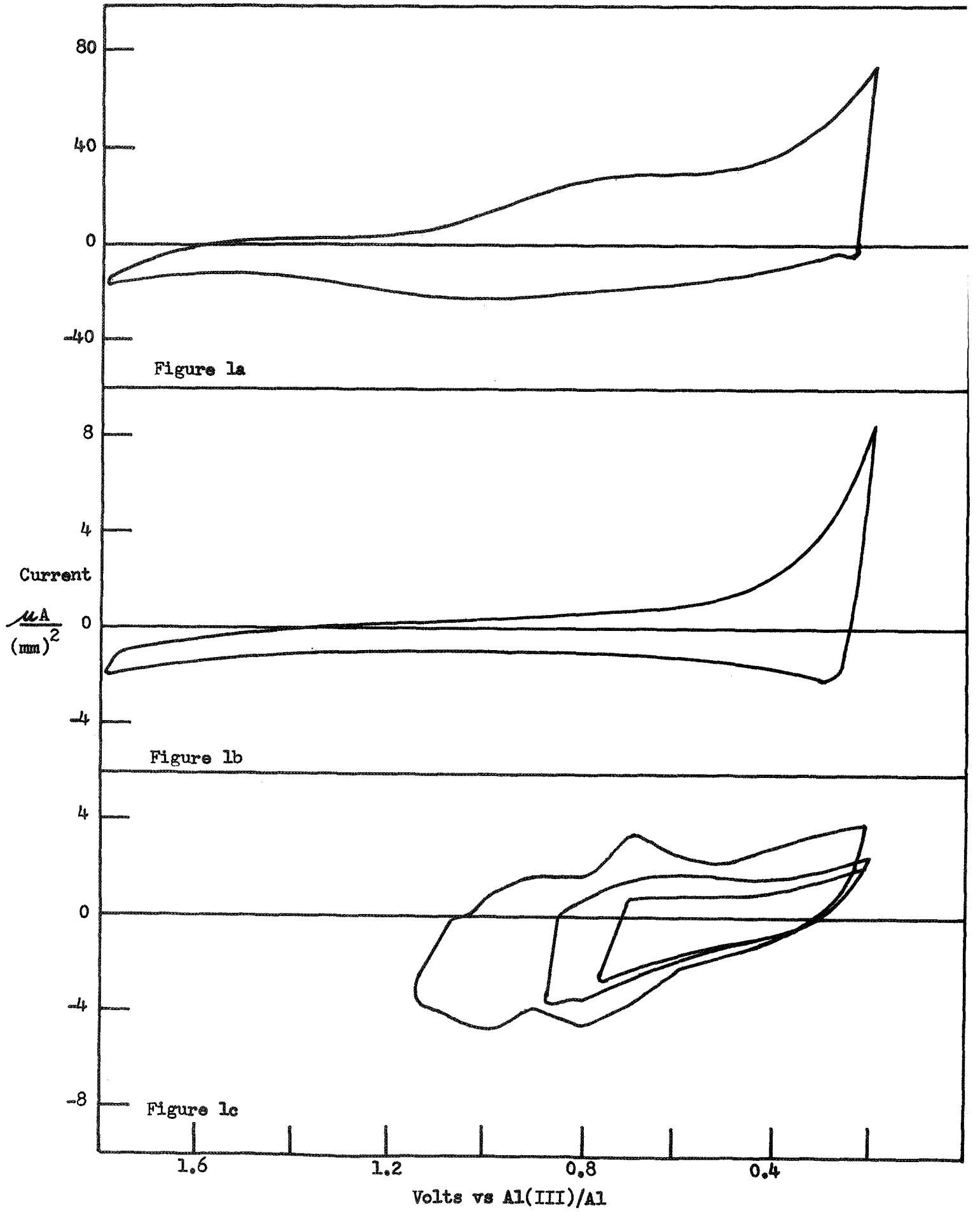
80
40
0
-40
Figure 1a
8
4
Current
μA
(mm)²
0
-4
Figure 1b
4
0
-4
-8
Figure 1c
1.6
1.2
0.8
0.4
Volts vs Al(III)/Al

Figure 2

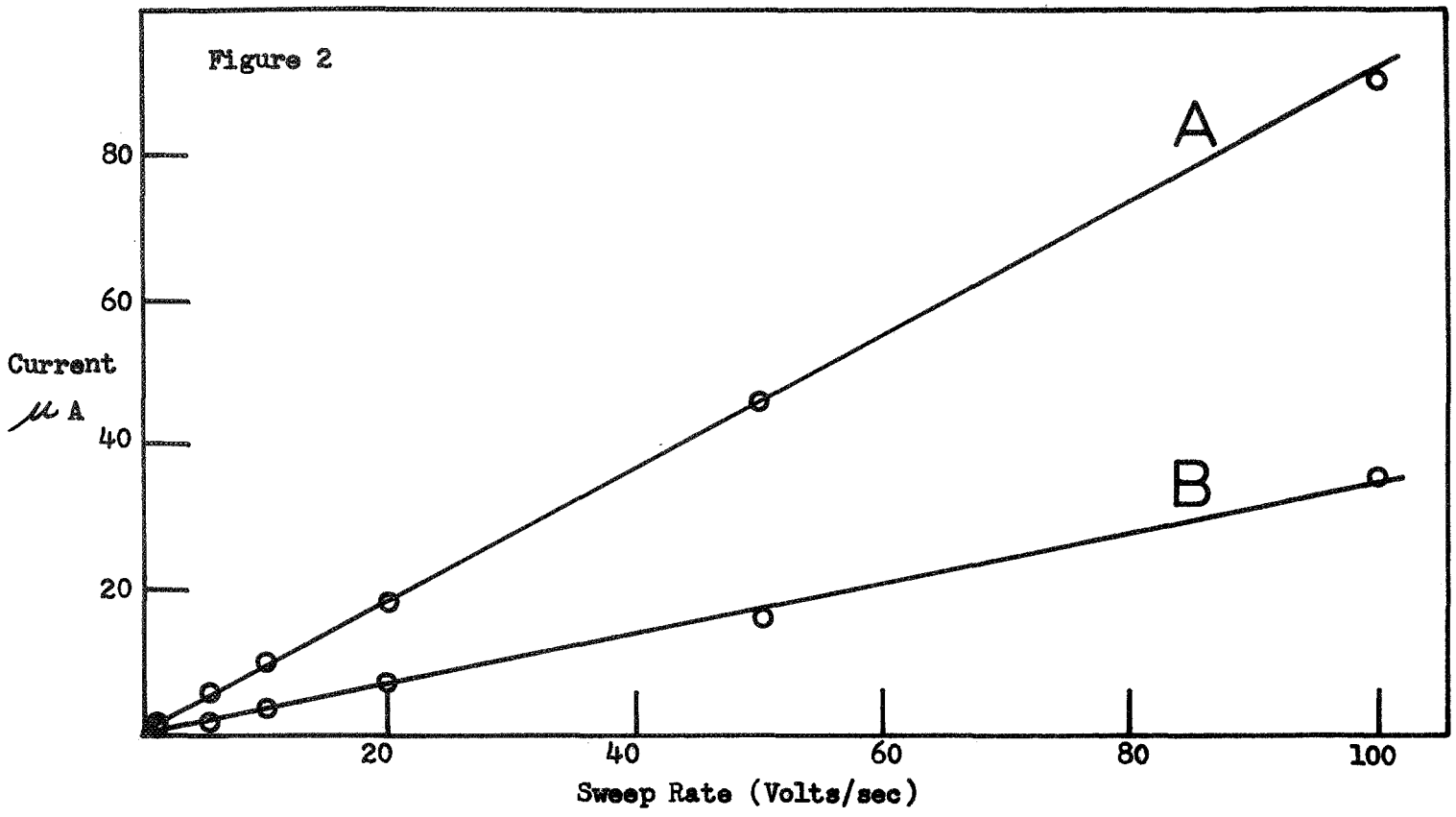

Figure 3

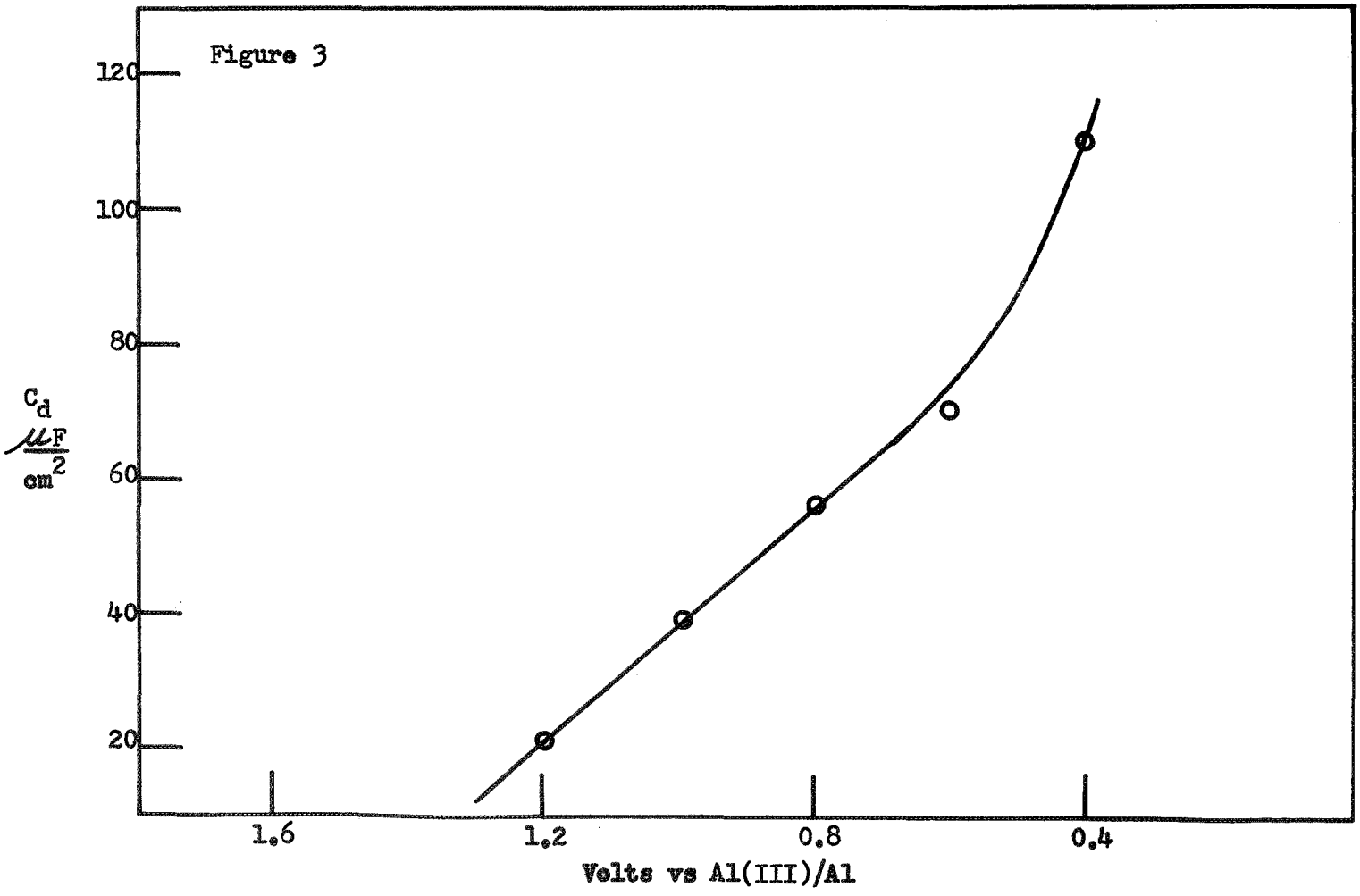

Figure 4

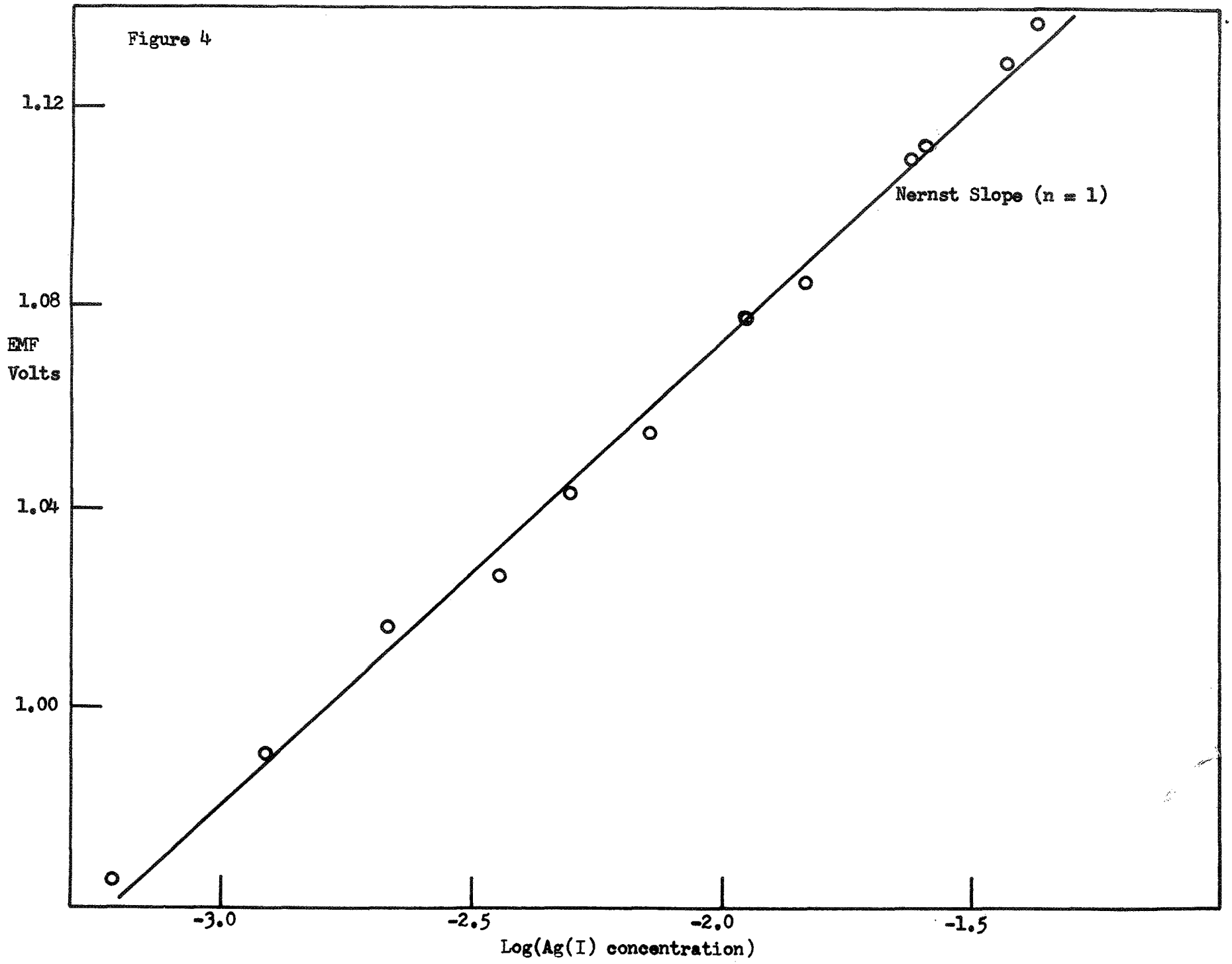
1.12
1.08
1.04
1.00
EMF
Volts
Nernst Slope (n = 1)
-3.0
-2.5
-2.0
-1.5
Log(Ag(I) concentration)

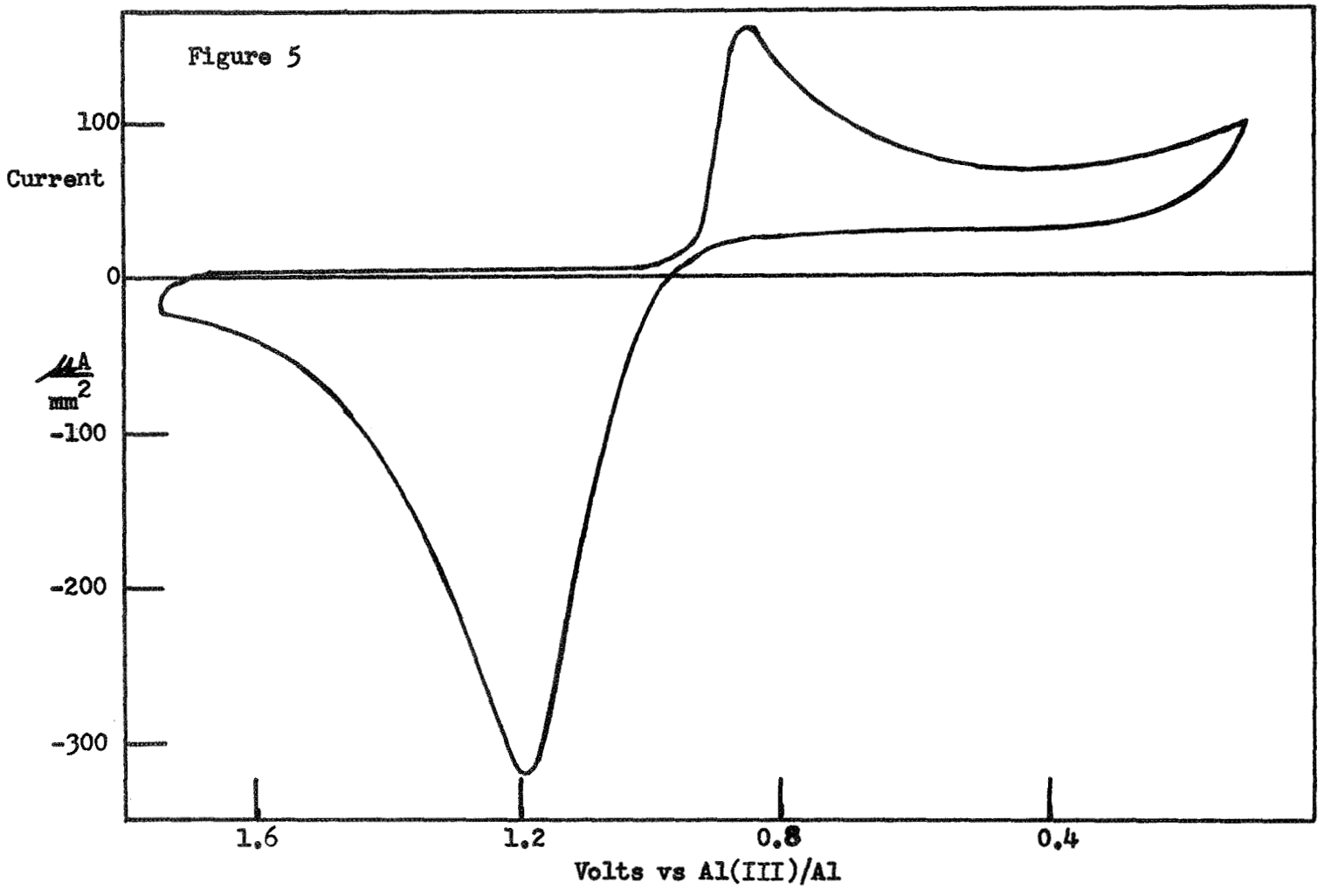
Figure 5
100
Current
0
μA/mm²
-100
-200
-300
1.6
1.2
0.8
0.4
Volts vs Al(III)/Al

Figure 6

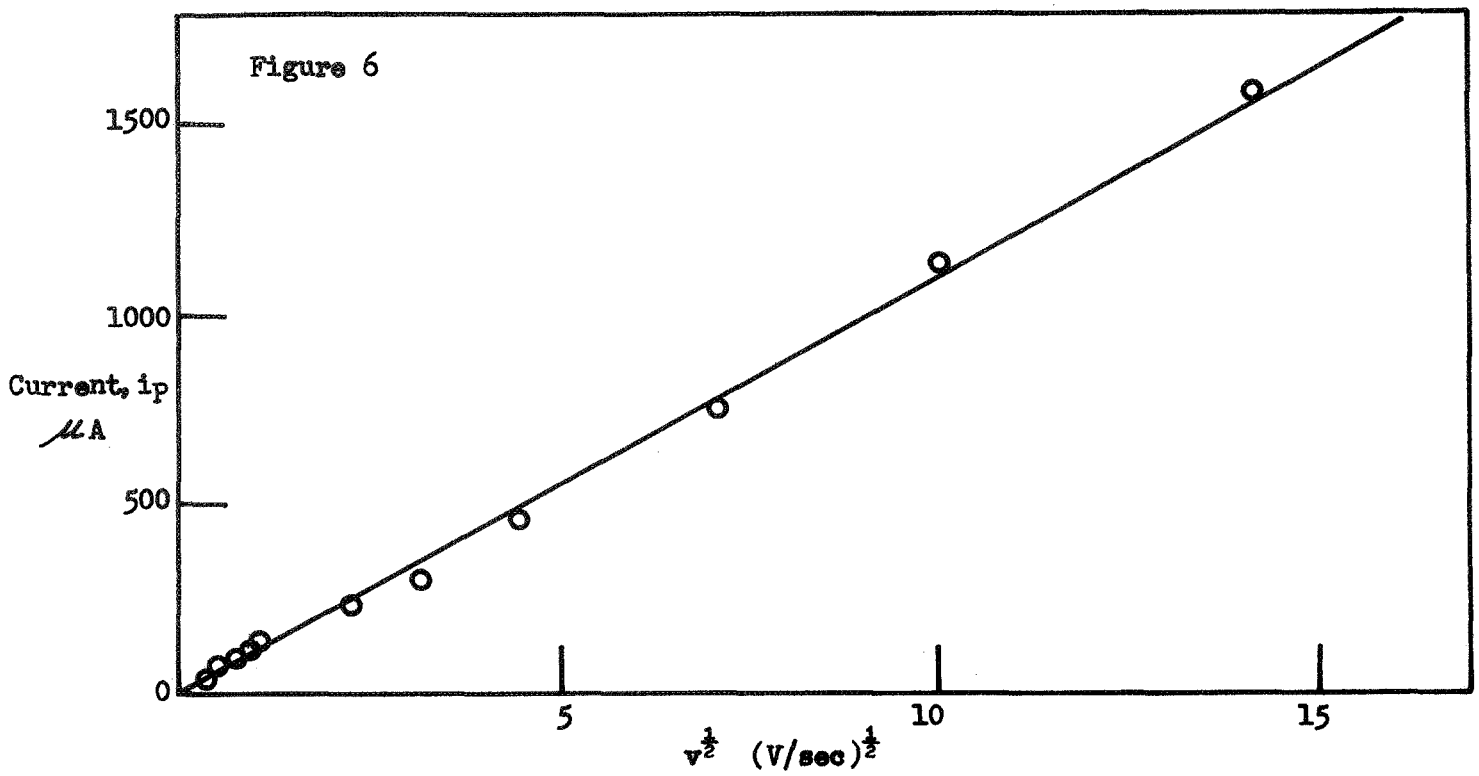

Figure 7

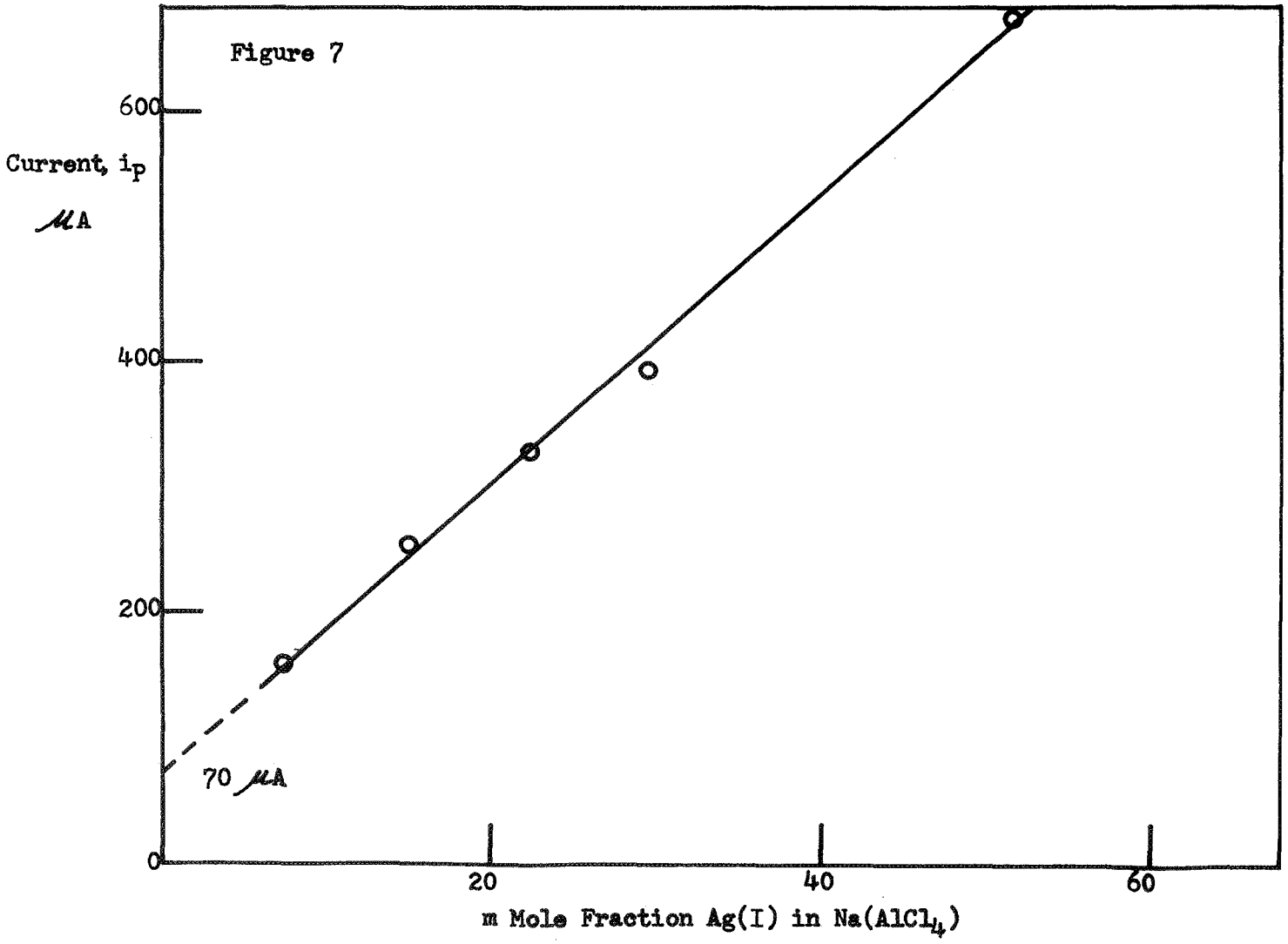

Figure 8

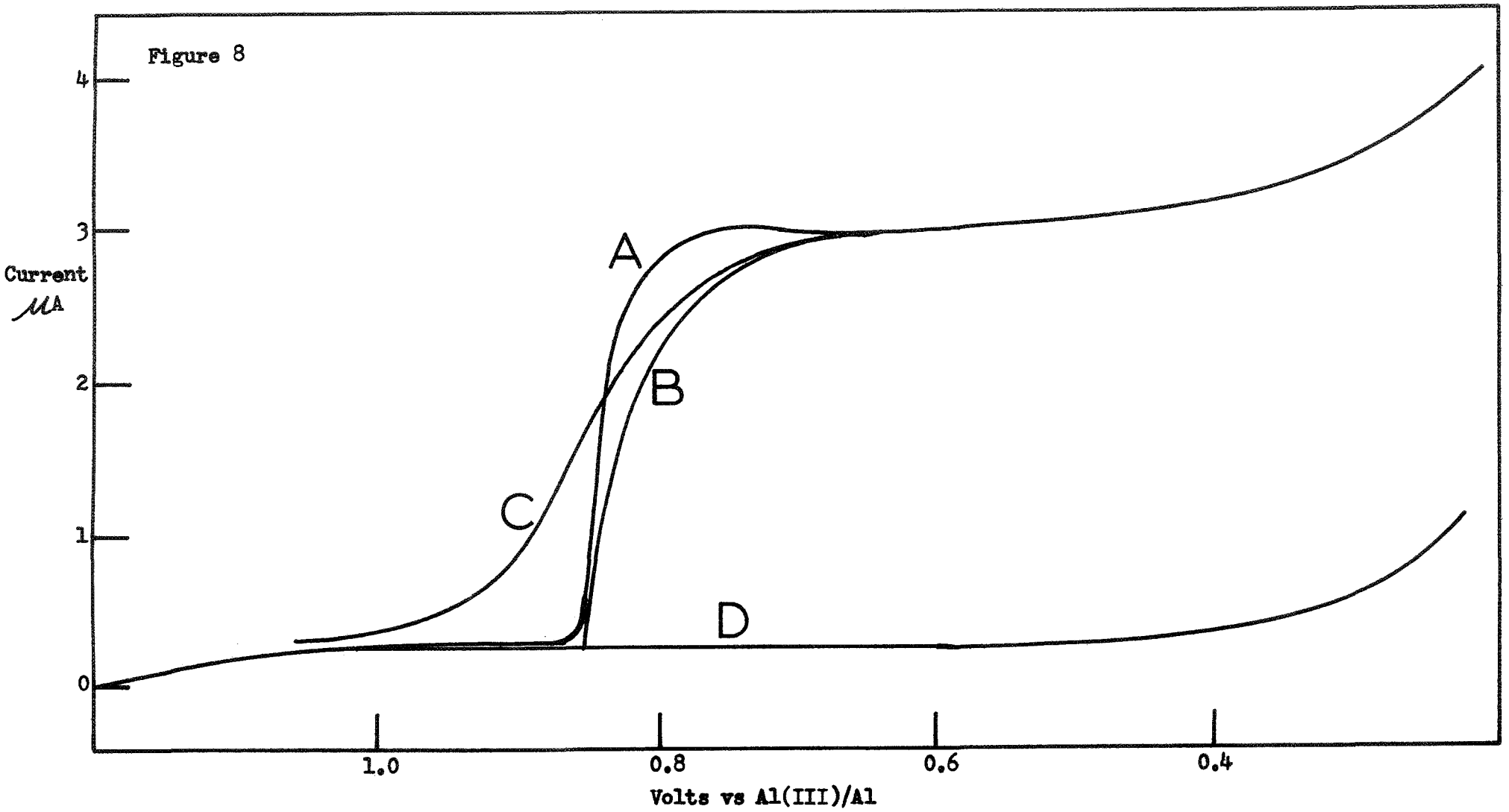

Figure 9

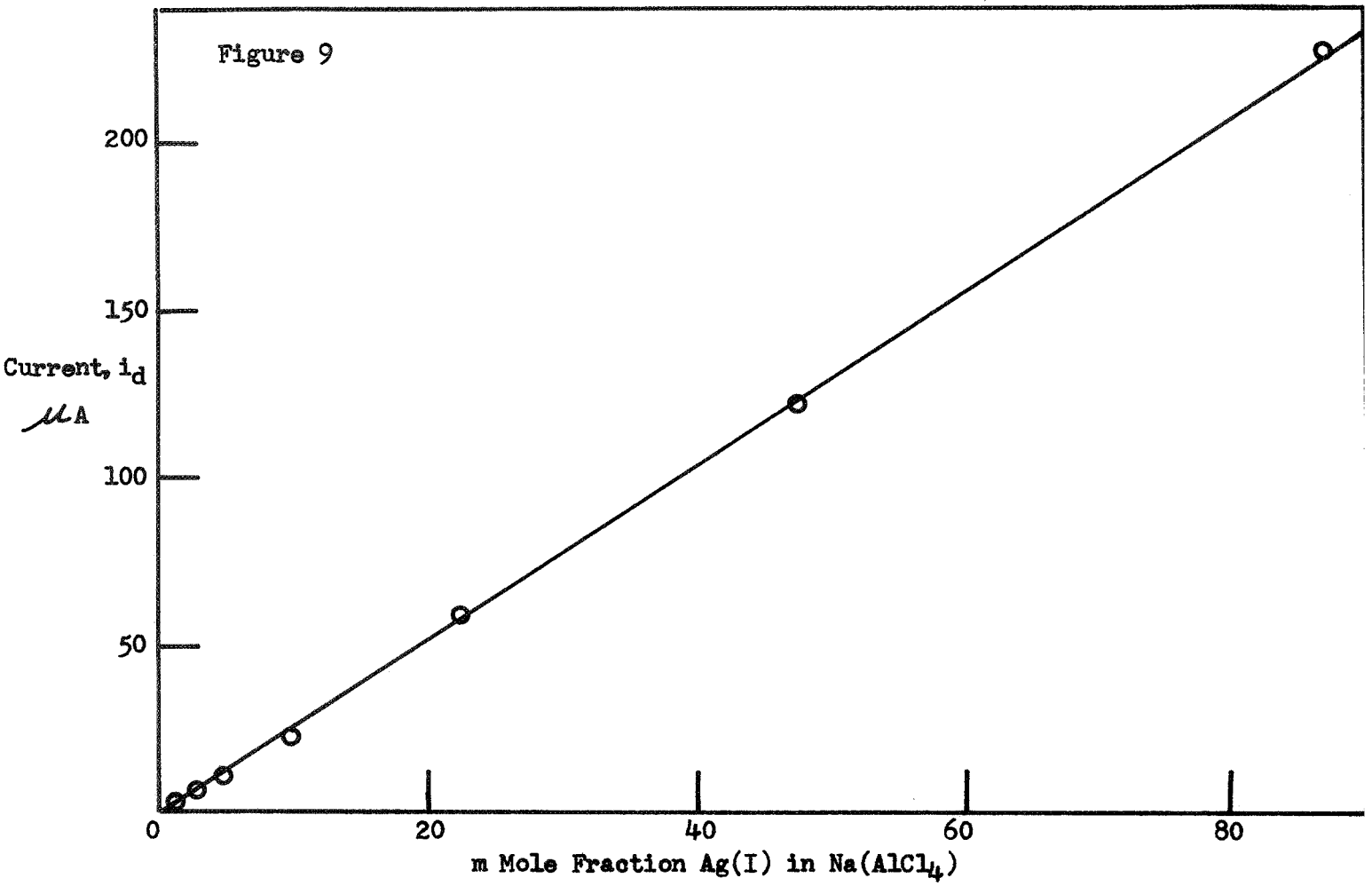

Figure 10

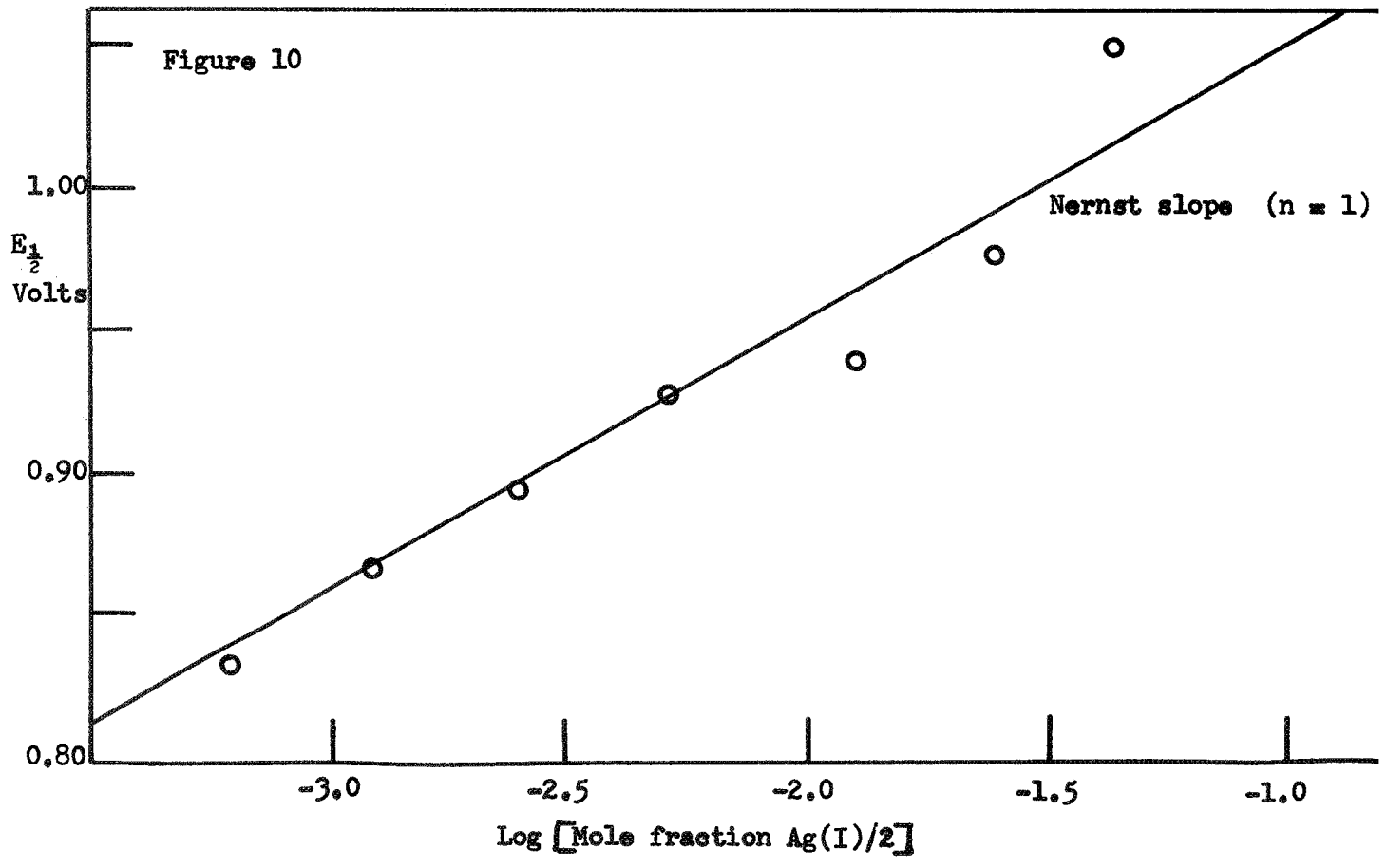

Figure 11

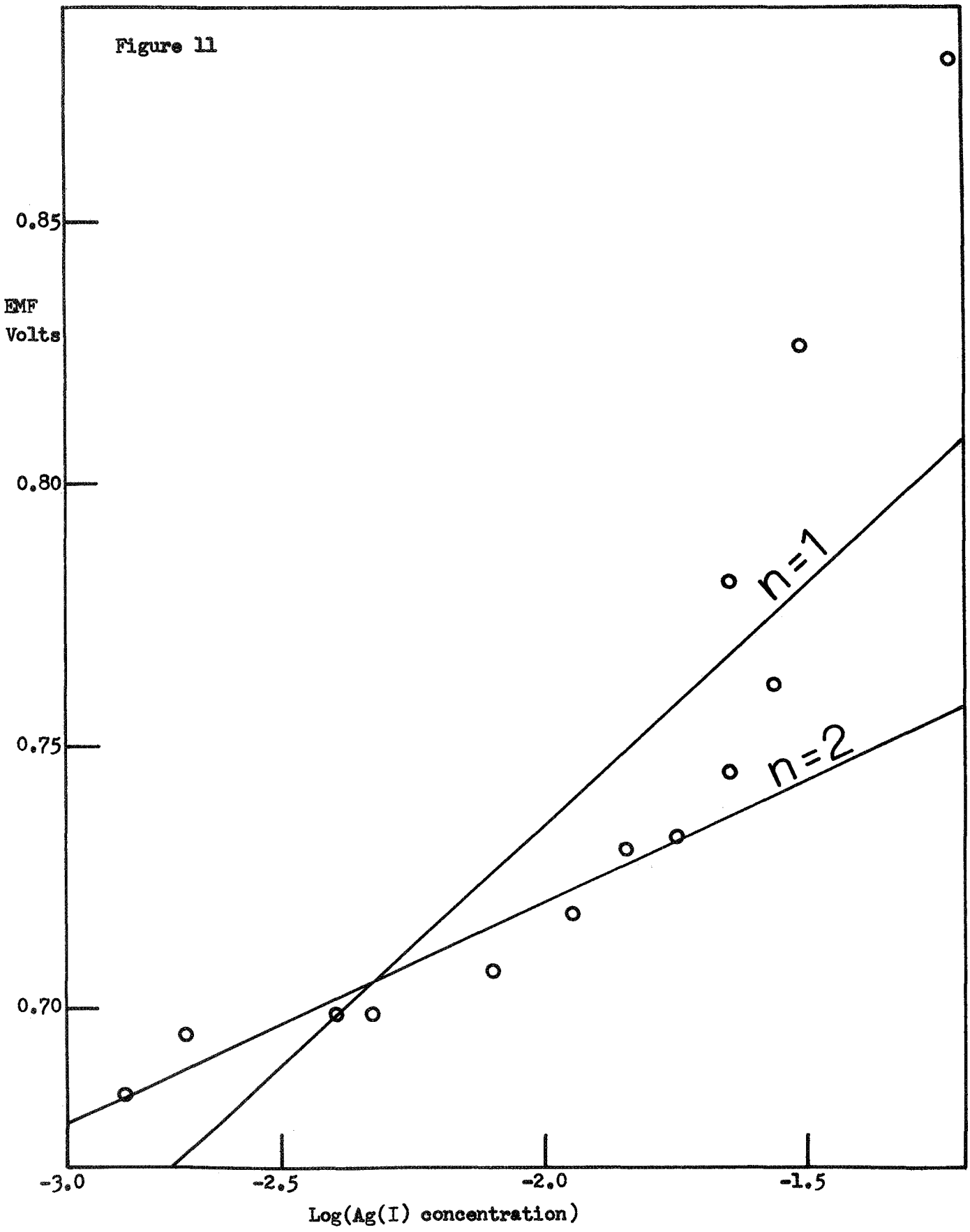
0.85
EMF
Volts
0.80
0.75
0.70
n=1
n=2
-3.0
-2.5
-2.0
-1.5
Log(Ag(I) concentration)

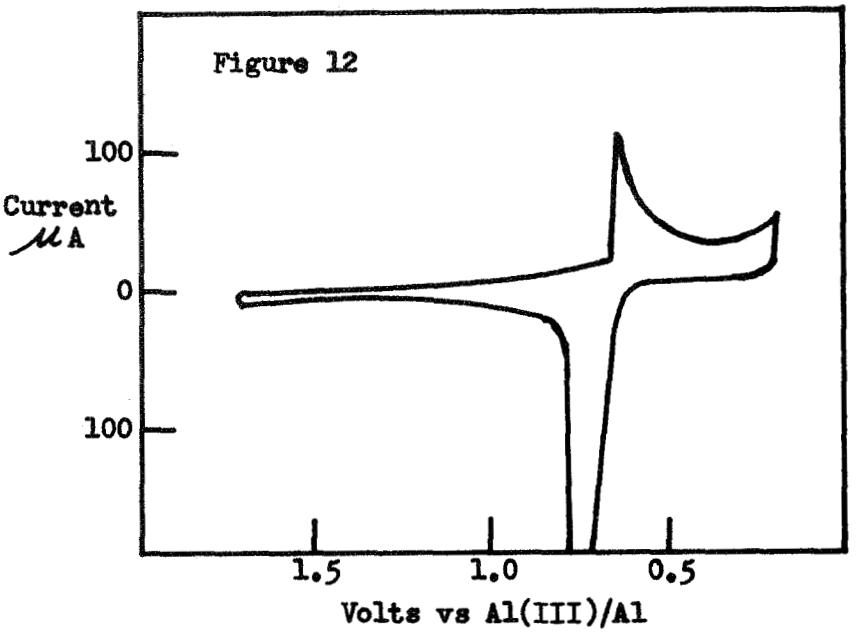
Figure 12
100
Current
μA
0
100
1.5
1.0
0.5
Volts vs Al(III)/Al

Figure 13

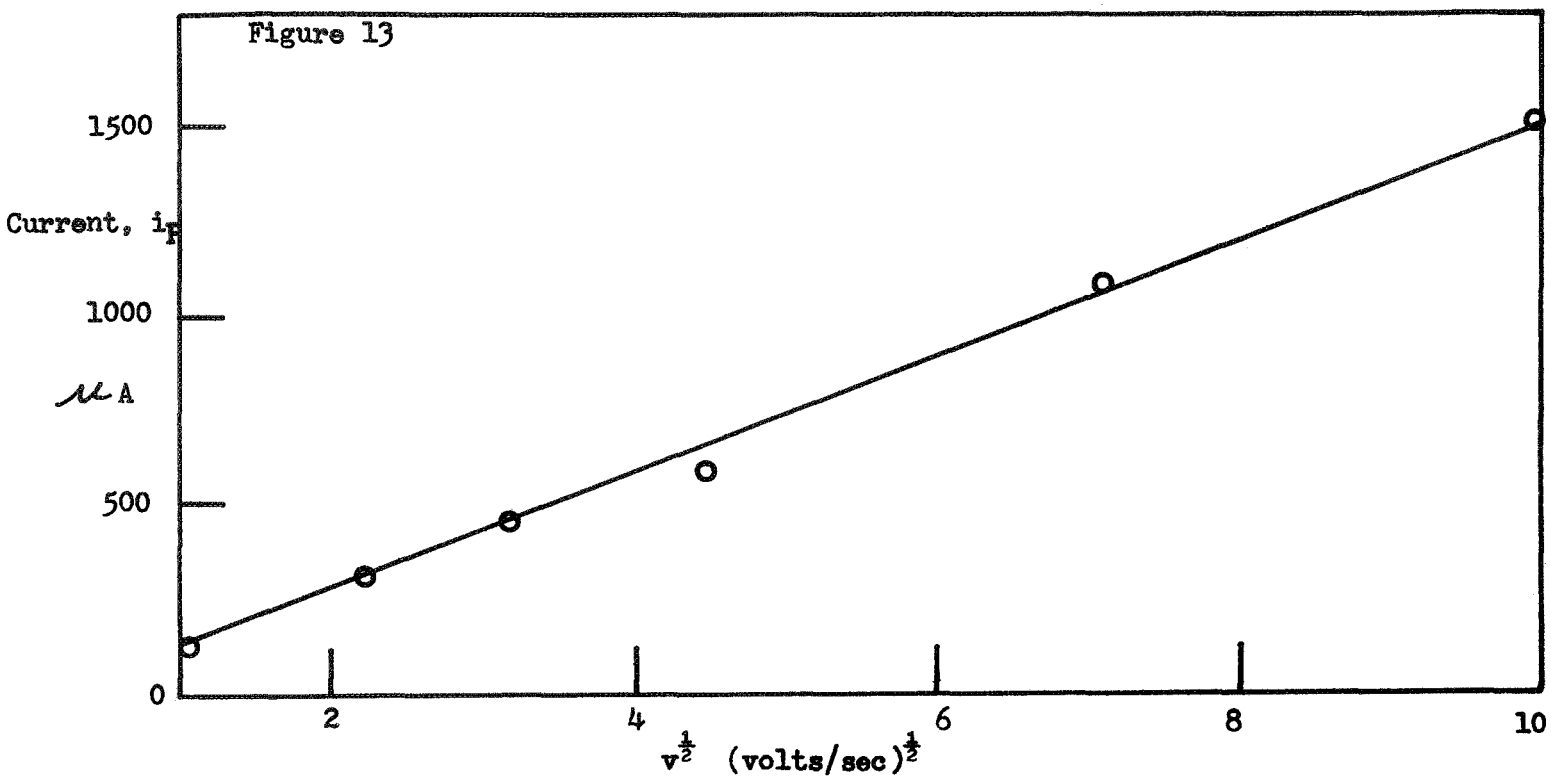

Figure 14

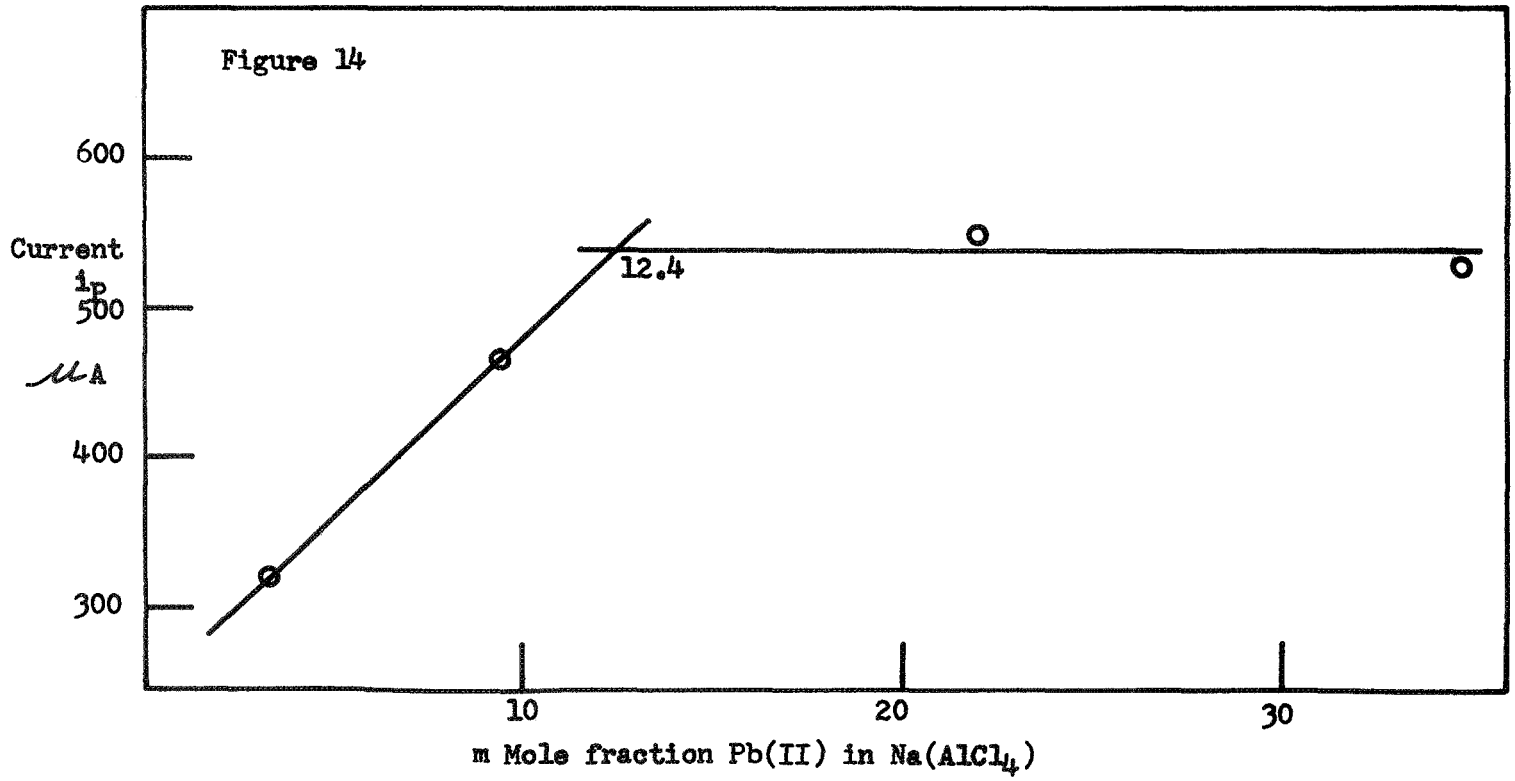

```
Input clock cycle in milliseconds
.1
input:  output volt div fact
6.1Ø7
input: N for normal
D for deriv
Q for spec
D
input R(M) in OHMS
Range and incr in volts
1ØØØØ
.6,.Ø1
full scale current is +Ø.1ØØØØØØE+Ø4 microamps
input:  pulse ht in volts
.Ø5
input:dly T & pulse W in mlsec
25Ø,25
set X and Y full scale
press key
set X and Y to calib
press key
input: X SC mks in volts
Y SC mks in mcamps
.1,1ØØ
set init pdt and ck drop knocker
press key
input: scale factor, 1 bias, & ave no
1Ø,Ø,5
```

Figure 15.

```
Input:  clock cycle in milliseconds
.1
input: output volt div fact
6.1Ø7
input: RM in OHMS
1ØØØ
full scale current is+Ø.1ØØØØØØE+Ø5 microamps
input: type of exp, N or S
S
input:  range in volts
.6
input: step ht in volts
.Ø1
input:  pulse ht in volts
.Ø5
input: step width, meas time in mlsec
5Ø,2Ø
set X&Y full scale
press key
set X&Y to zero
press key
input: X sc mks in volts, Y sc mks in mcamps
.1,1ØØØ
set init potential
press key
input curr sc fact, 1 bias, and ave no
1Ø,Ø,5
input: wait time
1ØØØØ
```

Figure 16.

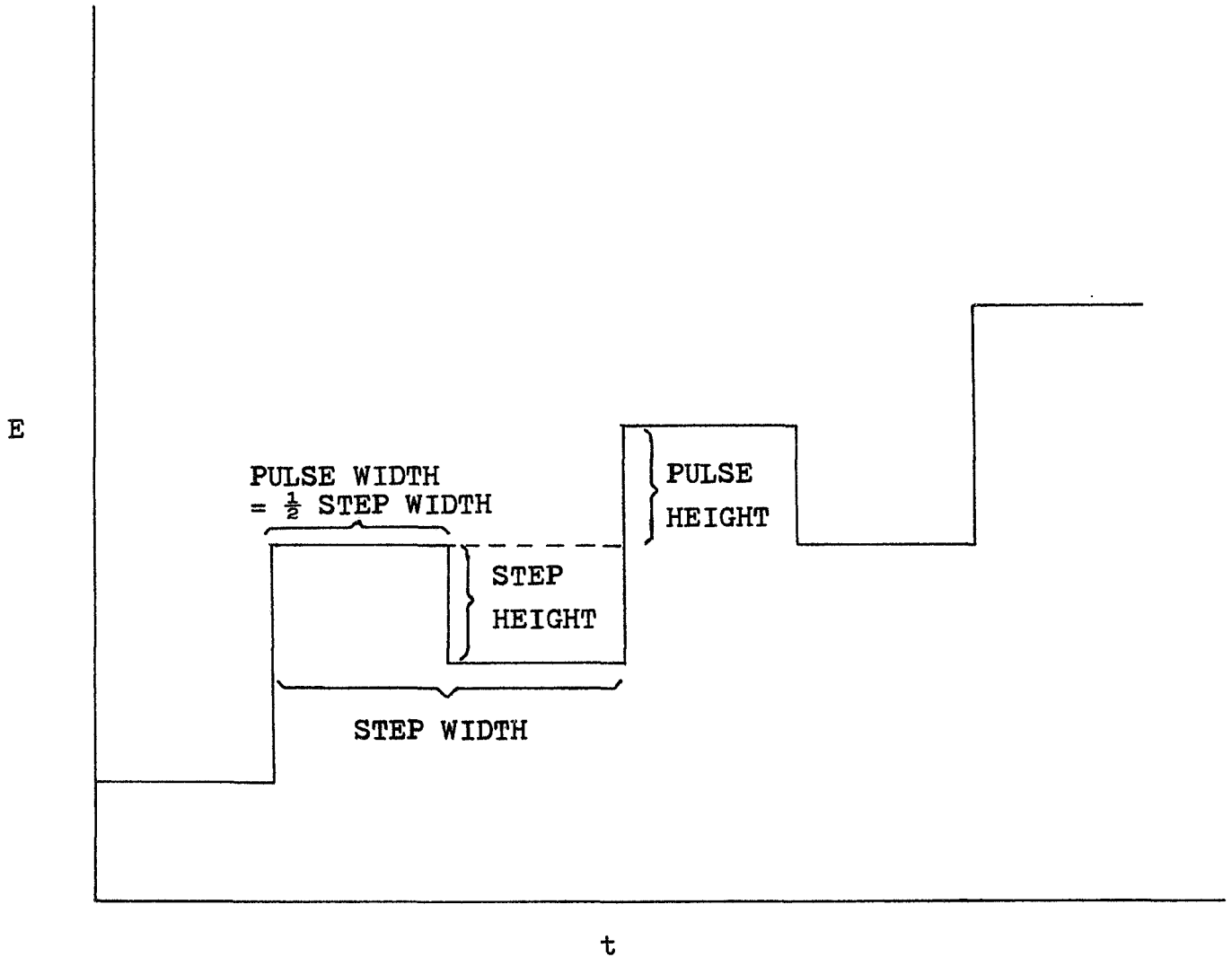
E
PULSE WIDTH
= ½ STEP WIDTH
PULSE
HEIGHT
STEP
HEIGHT
STEP WIDTH
t

Figure 17

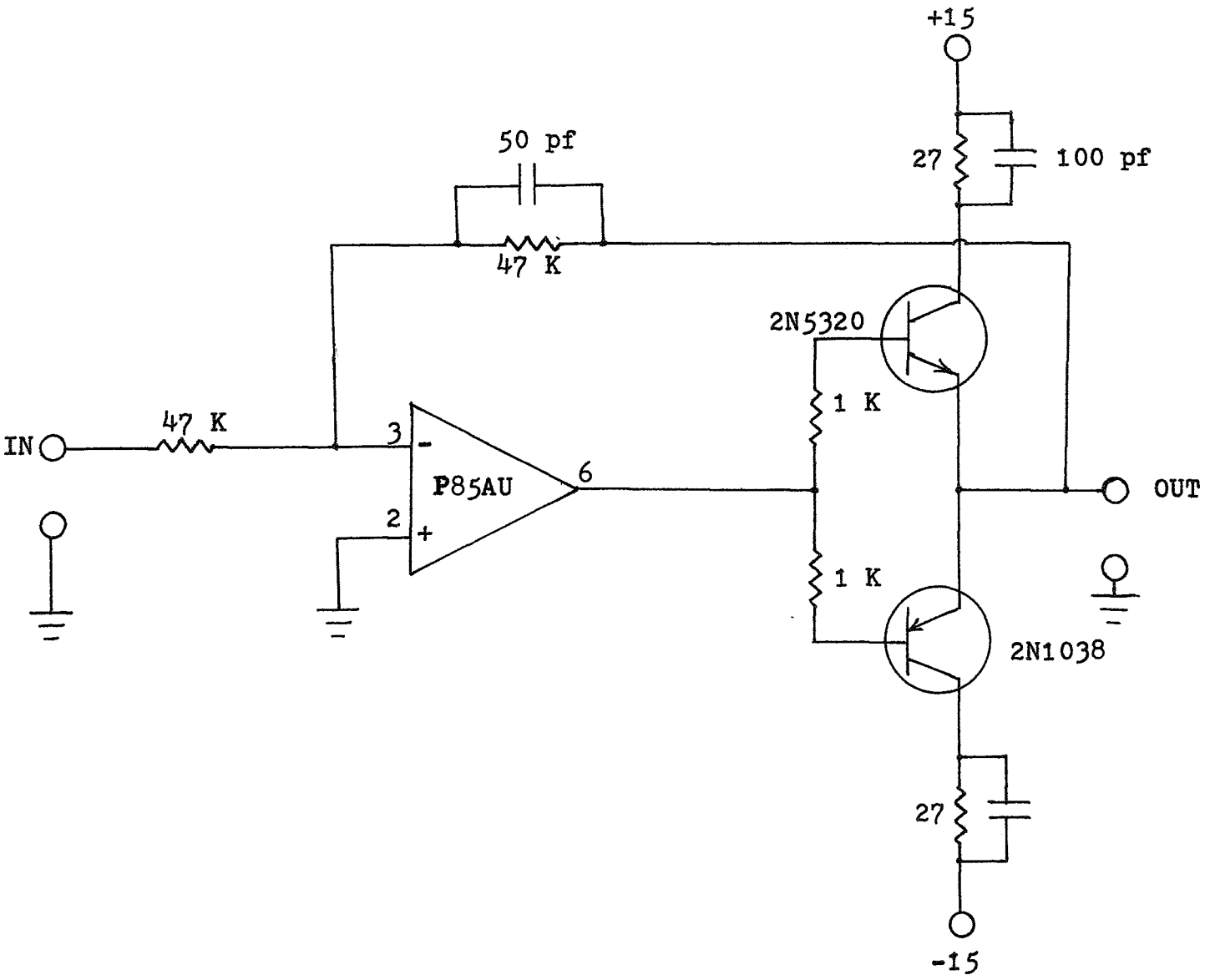
+15
50 pf
27
100 pf
47 K
2N5320
1 K
IN
47 K
3
-
P85AU
6
OUT
2
+
1 K
2N1038
27
-15

Figure 18

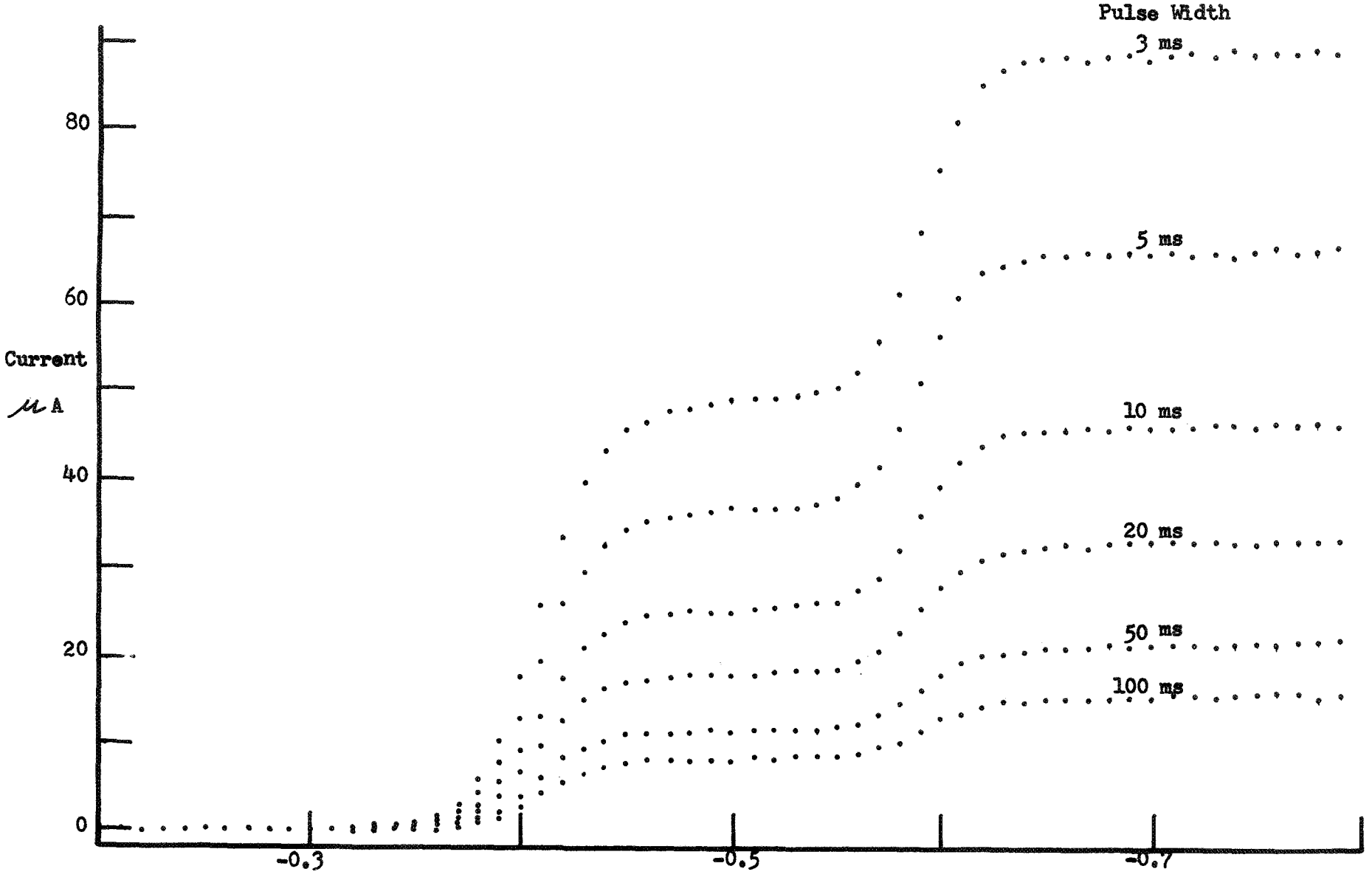
Pulse Width
3 ms
5 ms
10 ms
20 ms
50 ms
100 ms
80
60
40
20
0
Current
μA
-0.3
-0.5
-0.7
Volts vs SCE

Figure 19

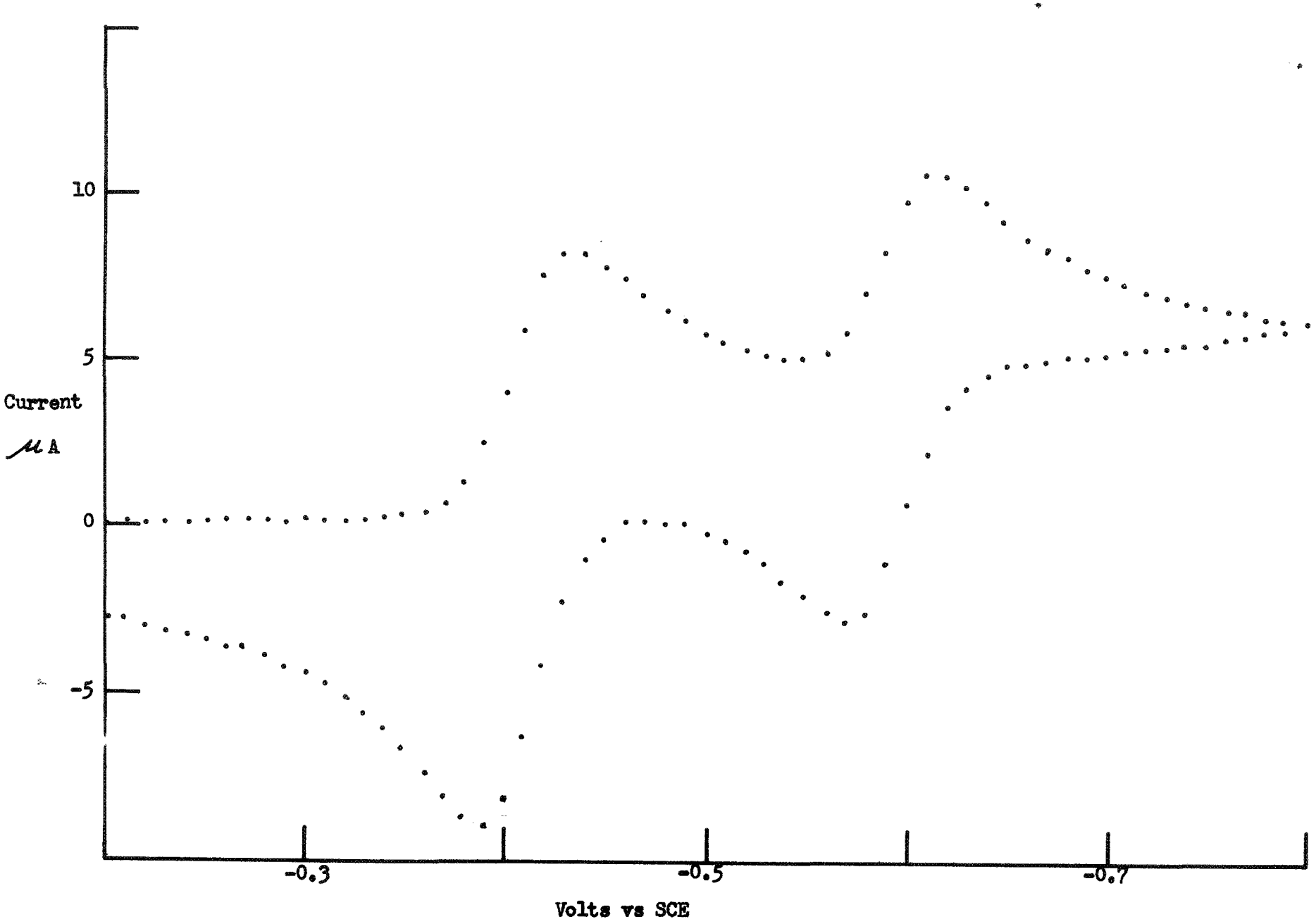

Figure 20

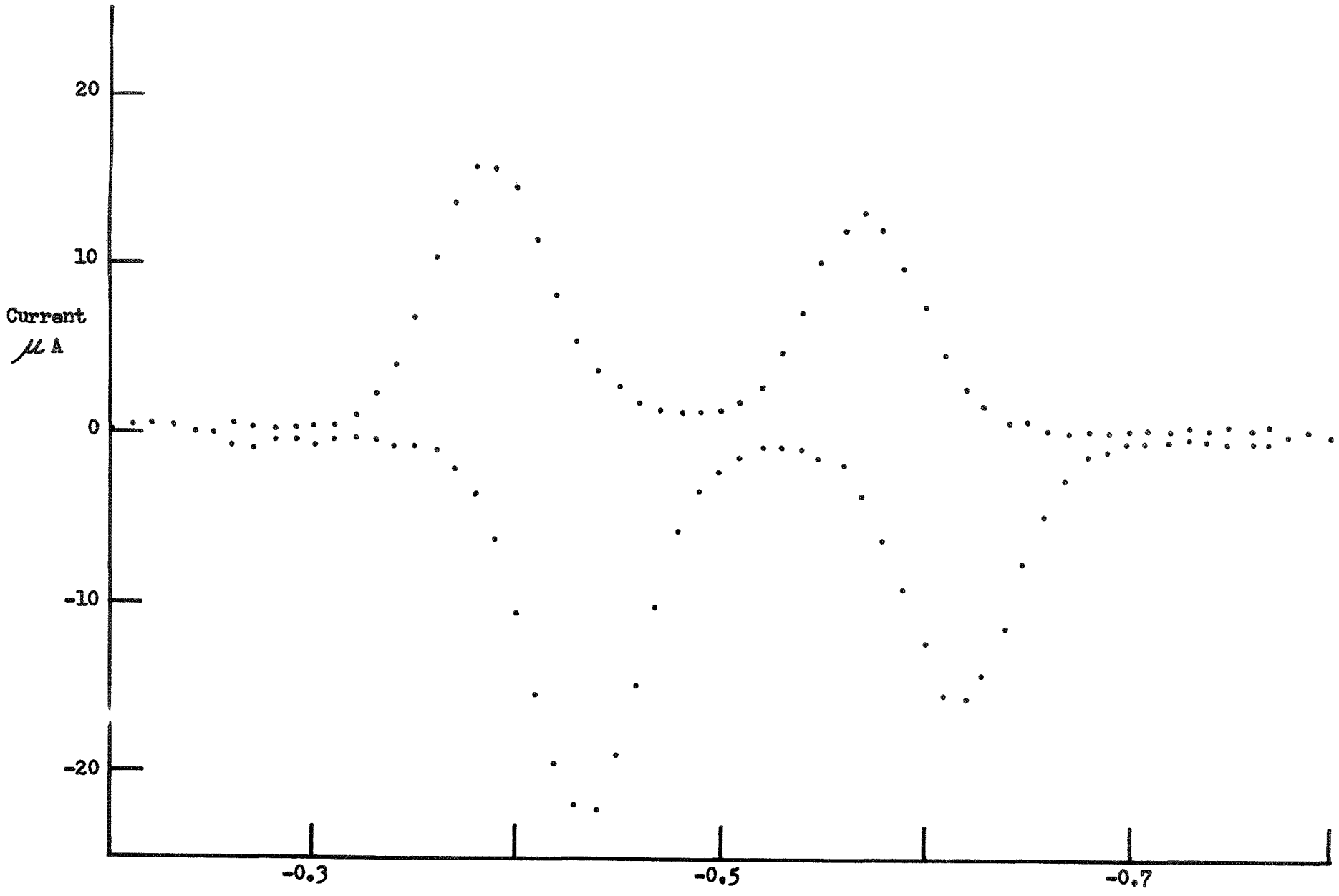

Figure 21